Studies on Galaxy Evolution: Morphology- Population Connection

A thesis submitted to the

University of Calicut, Kerala for the award of the

Degree of **DOCTOR OF PHILOSOPHY**

in **PHYSICS**

under the Faculty of Science

by

Aswathy. S

Department of Physics

University of Calicut

Kerala, India

October 2018

"To confine our attention to terrestrial matters would be to limit the human spirit"
—Stephen Hawking

Dedicated to my beloved master
Shri Kamlesh. D. Patel (Daaji)

CERTIFICATE

This is to certify that the thesis entitled "**Studies on galaxy evolution: Morphology- population connection**" submitted to the Department of Physics, University of Calicut by **Mrs. Aswathy. S** in partial fulfilment of the requirements for the award of the degree of **Doctor of Philosophy** is the original work carried out by her under my supervision and guidance at the Department of Physics, University of Calicut. No part of this thesis has been included previously for the award of any other degree, either in this university or any other institution. The thesis has been checked for plagiarism, using the *URKUND* software, at the CHMK library, University of Calicut and the similarity index is found within the permissible limit. Also, no changes were suggested by the thesis referees after evaluation, and therefore, there are no further corrections to be made in this thesis.

Supervisor:
Dr. C. D. Ravikumar
Associate Professor
Department of Physics
University of Calicut

DECLARATION

*I hereby declare that the thesis titled "***Studies on galaxy evolution: Morphology-population connection***" is an authentic record of research work carried out by me at the Department of Physics, University of Calicut under the supervision of Dr. C. D. Ravikumar. No part of this thesis has been included previously for the award of any other degree, either in this university or any other institution. The thesis has been checked for plagiarism, using the URKUND software, at the CHMK library, University of Calicut and the similarity index is found within the permissible limit.*

Date:

Aswathy. S

Research scholar

Department of Physics

University of Calicut

Contents

List of Tables

List of Figures

Acknowledgement

I had always been fascinated by astronomy and thankfully, at the end of a comparatively long research period, I still remain fascinated by astronomy! I can fondly remember a great many people who helped me to stay so and I am glad of a chance to thank them all. First and foremost, I would like to thank my supervisor Dr. C. D. Ravikumar for all his support and guidance throughout my research work. He is the first person to have introduced me to Astronomy during my post graduation years. I am thankful for his complete confidence in me without which I would never have been able to complete my work. As a guide, he is the best as he gives complete freedom to his students.

I am lucky to have been a student of the Department of Physics, University of Calicut which is well known for its eminent faculties. I fondly remember my teachers Dr. B. R. S. Babu and Dr. Vishnu Mayya Bannur for the infinite affection and guidance bestowed upon me ever since I stepped into this Department. I also take this opportunity to thank my teachers Dr. P. Rameshan, Dr. George Varghese and Dr. K. M. Varrier for their valuable lectures. All of them inspired me a lot in taking up my research work. I thank the present head of the Department Dr. P. P. Pradyumnan for his unconditional support in all matters associated with the submission of my thesis. I would like to thank all the other faculties of this department for their support and inspiration. I am thankful towards the present and past members of the department's office for the assistance provided during my work. I also thank KSCSTE for the fellowship I enjoyed during the research.

I can never find the right words to thank my fellow researchers in astronomy. I thank Dr. Jithesh for teaching me data analysis techniques and his ever flowing support throughout my research work. I am fortunate to have had a senior like

Dr. Dhanya and I owe many memorable moments during my research work to her love and support. I also thank Preetha and Nikesh for the assistance and support I received from them during the early days of my research. I am greatly indebted to my juniors Sitha, Vinod, Sruthi, Baheeja and Habeeb for enlivening the last few years of my research work with fruitful and interesting discussions. I thank all the research scholars in this Department for being good friends and wonderful colleagues. Special thanks to Arjun for extending a helping hand with the technicalities of my research work whenever I needed it and being a brother. Words fail me when I attempt to thank my dearest Jisha chechi for extending her valuable friendship upon which I could always rely. I can never thank her enough for the joyful moments we shared over these years. I am really blessed with a handful of friends whose company I cherish the most and I wish to thank every one of them.

I have no idea how to thank my family for their infinite support and unconditional love. My parents are the best in the world and they never seem to lose their faith in me. I am also blessed with a sister and brother who would never let me down. I thank my brother in law and fondly remember that he gifted me the laptop which remained my constant companion throughout the research period. Special thanks to my nephew Rohan for cheering me up whenever I was feeling low. I am blessed with immensely supporting in-laws and I can only thank God for it. My husband's parents would go out of their way to support my work and I shudder to think about what would I have done without them.

At last but never the least, I would like to thank my husband for being my strength and inspiration. He would console when one would expect him to complain and always manage to cheer me up. I am lucky to have my beloved son Sidharth and I am extremely thankful to him for being asleep whenever his mom had work to finish! I am sure I must have missed out someone and hence, I once again thank one and all who helped me complete this work.

List of Publications

1. **S. Aswathy** and C. D. Ravikumar
   "Study of central light concentration in nearby galaxies", *Monthly Notices of the Royal Astronomical Society* , 477 (2018), 2399-2405.

2. **S. Aswathy**, C.D. Ravikumar, V. Jithesh, Preetha A.U. and Dhanya Joseph
   "Stellar Population Synthesis of Bright X-ray Point Sources in NGC 1399", *Research Journal of Recent Sciences* , 3 (2014), 86-88.

3. **S. Aswathy**,C.D Ravikumar, A.U Preetha, V. Jithesh and Dhanya Josep
   "Optical Properties of Bright X-ray Sources in NGC 1399: Colour-X-ray Luminosity Correlation", *International Journal of Scientific & Engineering Research*, 5 (2014), 281-283.

4. **S. Aswathy** and C. D. Ravikumar
   "Co-evolution of nuclear rings, bars and the central intensity ratio of their host galaxies", *Under review in RAA*.

List of conference presentations

1. "Estimating the masses of super massive black holes using central intensity ratio", S. Aswathy and C. D. Ravikumar, 35th Annual Meeting of the Astronomical Society of India(ASI), 5-9 February 2018, Osmania University, Hyderabad.

2. "Study of central intensity ratio in nearby galaxies", S. Aswathy and C. D. Ravikumar, Regional Astronomy Meeting-IV, 1-2 December 2017, WMO Arts & Science college, Muttil, Wayanad.

3. "Study of central concentration in nearby galaxies", S. Aswathy, K.S Anju, Dhanya Joseph and C. D. Ravikumar, National Space Science Symposium (NSSS 2016), 9-12 February, 2016, VSSC, Thiruvananthapuram.

4. "Study of central concentration in early type galaxies", S. Aswathy, K. S. Anju, Dhanya Joseph and C. D. Ravikumar, 28th Kerala Science Congress, 28-30 January 2016, University of Calicut.

5. "Analysis of the Optical Counterparts of the X-ray point Sources in early type galaxies", S. Aswathy, C. D. Ravikumar, V. Jithesh, A. U. Preetha and Dhanya Joseph, 33rd meeting of Astronomical society of India (ASI), 17-20 February 2015, NCRA, Pune.

6. "Study of the optical counterparts of the X-ray point sources in early- type galaxies", S. Aswathy, C. D. Ravikumar, V. Jithesh, A. U. Preetha and Dhanya Joseph, Research in Astronomy: Opportunities and Challenges, 7-9 December 2014, Nirmala College, Muvattupuzha.

7. "Optical properties of bright X-ray point sources in NGC 1399: Colour X-ray luminosity correlation", S. Aswathy, C. D. Ravikumar, A. U. Preetha, V. Jithesh and Dhanya Joseph, International Conference on Recent Advances in Physics for Interdisciplinary Developments, 23-24 January 2014, Sathyabama university, Chennai, Tamil Nadu.

8. "Stellar population synthesis of bright X-ray point Sources in NGC 1399", S. Aswathy, C. D. Ravikumar, V. Jithesh, A. U. Preetha and Dhanya Joseph, 3rd International Science Congress Association, on 8-9 December 2013, Karunya University Coimbatore, Tamil Nadu.

9. "Stellar Population Synthesis of X-ray point sources in NGC 1399", S. Aswathy, C. D. Ravikumar, V. Jithesh, A. U. Preetha and Dhanya Joseph, Workshop on Astronomy Research: Opportunities and Challenges, 12-14 August 2013, MACFAST, Thiruvalla, Kerala

Constants and Abbreviations

Physical Constants

Parsec	$\mathrm{pc} = 3.086 \times 10^{18}$ cm
Solar Mass	$M_\odot = 1.989 \times 10^{33}$ g
Solar Luminosity	$L_\odot = 3.826 \times 10^{33}$ erg/s

Abbreviations

ACS	Advanced Camera for Surveys
AGN	Active Galactic Nucleus
ASCA	Advanced Satellite for Cosmology and Astrophysics
BHXB	Black Hole X-ray Binary
CIR	Central Intensity Ratio
FOV	Field Of View
HMXB	High Mass X-ray Binary
HST	Hubble Space Telescope
IMBH	Intermediate Mass Black Hole
IMF	Initial Mass Function
IR	Infrared
IRAF	Image Reduction Analysis Facility
LMXB	Low Mass X-ray Binary
NED	NASA/IPAC Extragalactic Database
NGC	New General Catalogue
ROSAT	Roentgen Satellite
SExtractor	Source Extractor
SMBH	Supermassive Black Hole

ULX	Ultraluminous X-ray Source
UV	UltraViolet
WFPC2	Wide-Field Planetary Camera 2
XRB	X-ray Binary

Chapter 1

Introduction

Astrophysics is one of the most popular branches of physics as it appeals to people of all age groups. Everyone is fascinated by the beautiful night sky. Man has always been curious about space. Astrophysics explores the physics behind celestial objects expanding its scope well beyond the part of the Universe visible to naked eyes. Our first telescope dates back to 1608 by Hans Lippershey of Netherlands. This was later modified by Galilio and he used it to discover the moons of Jupiter and closely observe the surface of the moon. Today, we have high resolution telescopes not only in ground but also in space enabling us to get a clearer and deeper view of the Universe.

The largest structures in space known to mankind are called galaxies. Though Messier identified some of the nearby galaxies in 1700, these were thought to be either clouds or group of stars residing in our own galaxy until the beginning of 19^{th} Century. In 1923, using the Hooker telescope situated at Mt. Wilson, Edwin Hubble discovered Cepheid variables in Andromeda galaxy. This discovery made it possible to measure the distance to this particular galaxy proving it to be too far away to be part of our own galaxy. Hubble is considered as one of the greatest astronomers of all times as he led many crucial discoveries in astronomy. His contribution to the studies on galaxy evolution is highly significant. He put forward the first ever morphological classification of galaxies which is discussed in the next section.

1.1 Hubble's classification of galaxies

Hubble introduced his morphological classification of galaxies in the book titled 'The Realm of the Nebulae' in 1936. His classification scheme is widely known as the Hubble's tuning fork diagram as the arrangement of galaxies resembles a tuning fork as shown in Figure 1.1. His classification scheme includes elliptical, lenticular, spiral and irregular galaxies. Elliptical galaxies are placed on the left side of the fork and arranged on the basis of their increasing ellipticity. The galaxies which are round are termed as E0 whereas the most elliptically shaped galaxies are denoted by E7. Spiral galaxies are classified based on the presence or absence of bars and arranged on the two arms of the fork accordingly. Lenticular galaxies (S0s) are placed between ellipticals and spirals. All other galaxies with peculiar shapes are called irregulars.

Generally, a galaxy is known to be consisting of mainly three components: bulge, disc and halo. The central spheroidal part of a galaxy is termed as the bulge, the flattened structure surrounding it is called the disc and the halo is believed to contain old stellar clusters and dark matter. The morphological classification of galaxies is linked with the presence of each of these components in them. Elliptical galaxies are bulge dominated systems, spirals are dominated by discs and lenticulars contain a spheroidal bulge along with a disc surrounding it. This hints at an association of morphology of galaxies and stellar population. Further, Hubble proposed that his arrangement of galaxies is related to their evolution implying that the elliptical galaxies which are situated at the left hand side of the tuning fork gradually evolved to form spirals located at the arms of the fork. Hence the ellipticals and lenticulars situated at the left side are termed as early-type galaxies and the spirals on the right side are called late-type galaxies. Though this no longer seems to be correct, early-type and late type galaxies appear to have followed different ways in their formation and evolution. In this thesis, we explore this apparent connection between stellar population and their host galaxies using photometric techniques.

1.2 Motivation and outline of the thesis

Integrated photometric properties of galaxies are intimately connected with the different stellar population, star formation history and also the chemical evolution of the galaxy. With the advent of Charge Coupled Device (CCD) detectors and more sophisticated telescopes, there was a wealth of good quality photometric images especially of the galaxies in the nearby Universe. The photometric decomposition of the surface brightness distributions of these galaxies provided new insights into the formation and evolution of these galaxies. Multi- wavelength studies aided in resolving different components of galaxies such as X-ray point sources and star clusters. Studies on the central regions of galaxies revealed the presence of super massive black holes. Many of these studies hinted at the co-evolution of these objects with their host galaxies. Though this is hardly surprising, a deeper understanding of the complex relationship between each of these components can be crucial in unfolding the evolution of their host galaxies. In this light, we perform studies on nearby galaxies using photometric techniques.

We carry out studies on a group of galaxies which are morphologically similar and devise correlations between various parameters associated with the objects under study. We begin with the quest to identify the optical properties of bright X-ray point sources which are situated around the nearby galaxies. We try to understand their dynamical evolution through stellar population synthesis. This is followed by a study on the optical region hosting the most luminous X-ray source within a galaxy that is the central super massive black hole. In the final part of our work, we carry out photometric studies on the central region of a sample of spiral galaxies with nuclear rings and bars, yet another carriers of information regarding the evolutionary history of their host galaxies. We provide a quick overview of each of these works in this chapter and a short description follows.

In Chapter 1, we introduce the motivation with which we have undertaken the studies performed in this thesis. Our work may be divided into three parts: the first part is an optical study of X-ray point sources in nearby galaxies, the second part deals with the central light concentration in nearby galaxies and the final part discusses the co-evolution of nuclear rings, bars and the central intensity ratio of their host galaxies. Chapter 1 includes a quick literature review of all the three

works reviewing the scope of each of these works in the current scenario. We have also included a brief description of the types of softwares used in our analysis along with the telescopes which provided us with the data presented in this work.

The first part of this study deals with identifying the optical counterparts of bright X-ray sources in a sample of three galaxies namely NGC 1399, NGC 4552 and NGC 4649. Archival Chandra and Hubble Space Telescope (HST) images are used for the analysis. We find a strong correlation between X-ray luminosities and $F475W - F850LP$ colours for non-Ultra luminous X-ray sources (ULXs). The ULX sources clearly defy the correlation supporting the prediction that X-ray production mechanism in ULXs is different from that of the other bright X-ray sources in a galaxy. We attempt to explain how such a strong correlation seems to be imposing constraints on the evolution of stellar clusters hosting X-ray sources using population synthesis.

Further, we carry out the stellar population synthesis (SPS) of X-ray point sources in NGC 1399 with an aim to investigate the dependence of X-ray characteristics on the dynamical properties of the sources. Using the SPS code of Bruzual and Charlot 2003 (BC03) and magnitudes in four *HST* filters, we estimate the possible ages and masses of these sources. We find that their X-ray luminosities are anti-correlated with the derived stellar masses excepting the two ULXs, the Spearman's rank correlation coefficient being -0.62 with a significance greater than 99 percent. As the optical counterparts are definitely multiple sources (most likely globular clusters), the strong trend exhibited by X-ray sources suggests the possibility of existence of multiple sources for the production of X-rays as well. Further, SPS also shows that the brighter X-ray sources are in general younger. This work is summarised in Chapter 2.

In Chapter 3, we propose a novel technique to estimate the masses of super massive black holes (SMBHs) residing at the centres of massive galaxies in the nearby Universe using simple photometry. Aperture photometry using source extractor (SExtractor) is employed to determine the central intensity ratio (CIR) at the optical centre of the galaxy image for a sample of 49 nearby galaxies with dynamical SMBH mass estimations. We find that the CIR of ellipticals and classical bulges is found to be strongly correlated with SMBH masses whereas pseudobulges and ongoing mergers show significant scatter. Also, the CIR of low luminosity active galactic

nuclei (LLAGN) in the sample shows significant connection with the 5 GHz nuclear radio emission suggesting a stronger link between the former and the SMBH evolution in these galaxies. In addition, it is seen that various structural and dynamical properties of the SMBH host galaxies are correlated with the CIR making the latter an important parameter in galaxy evolution studies. We propose the CIR to be an efficient and simple tool not only to distinguish classical bulges from pseudo bulges but also to estimate the mass of the central SMBH.

In the last part of the work which is described in Chapter 4, we carry out a study on the central regions of nearby spiral galaxies hosting nuclear rings using the method of CIR. We observe that the relative sizes and lengths of the semi major axis of nuclear rings strongly correlate with the CIR. These correlations suggest that the galaxies hosting smaller and denser nuclear rings may have little star formation near their centres as these tend to possess low values of CIR. This scenario appears to be a consequence of stronger bars as advocated by the significant connection observed between the CIR and bar strengths. The CIR can serve as a crucial parameter in unfolding the coupled evolution of bars and rings as it is intimately connected with both their properties. In Chapter 5, the entire work presented in this thesis is summarised and we discuss future scopes of the work.

The following section deals with the review of literature related to the first part of our work which is an optical study of X-ray sources in nearby galaxies.

1.3 Study of optical counterparts of bright X-ray sources in nearby galaxies

X-ray point sources in nearby galaxies have been extensively studied over the past three decades as observations of high spatial resolution were made available by *Chandra* X-ray Observatory. Among the X-ray point sources in nearby early-type galaxies (ETGs), the brightest sources were often identified to be low mass X-ray binaries (LMXBs; Trinchieri & Fabbiano, 1985; Sarazin et al., 2000). These are systems which host a neutron star or black hole possibly accreting gas from a companion star. An artist's impression of an X-ray binary (XRB) system consisting of an accreting compact object and its companion star is shown in Figure 1.2.

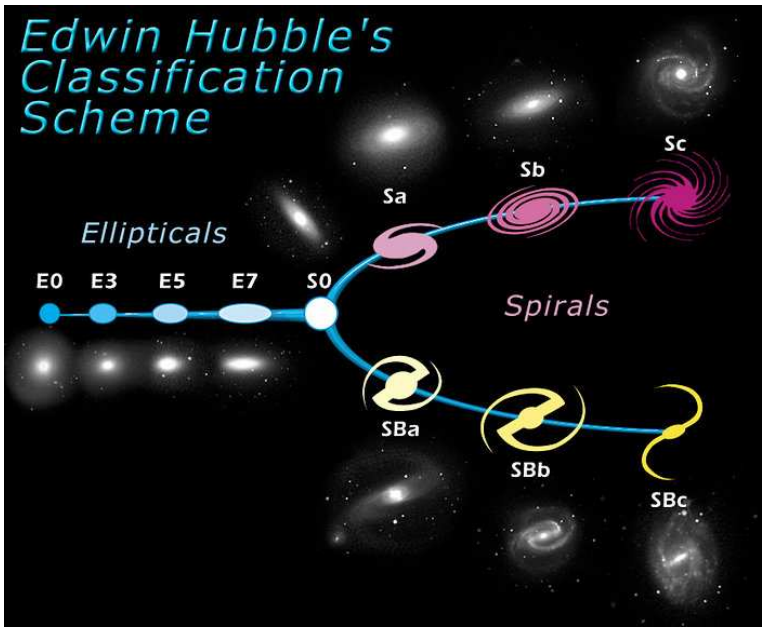

Figure 1.1: Hubble's tuning fork classification scheme of galaxies. Image Courtesy: **www.spacetelescope.org**

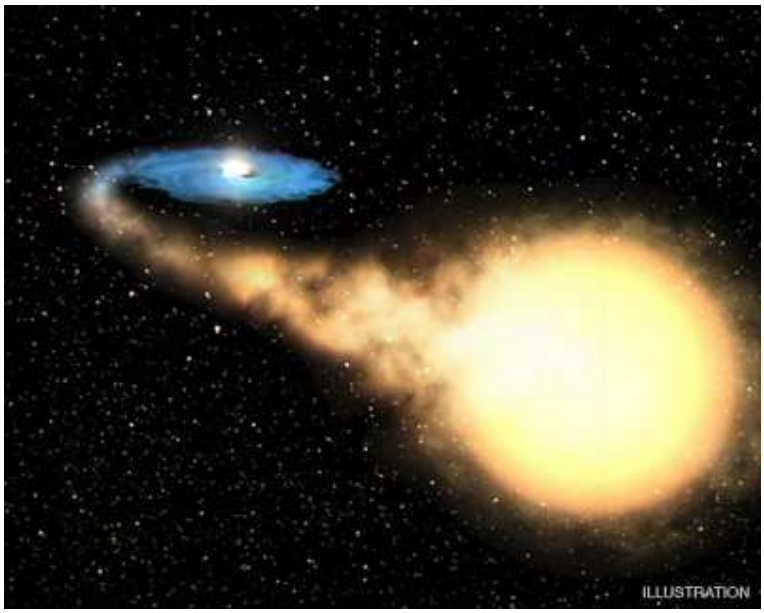

Figure 1.2: An artist's impression of an X-ray binary system consisting of an accreting compact object and its companion star. Image Courtesy: **www.chandra.harvard.edu**

Since it is possible to resolve these sources with the help of *Chandra*, highly resolved observations in *HST* can be used to study their optical counterparts. Such multi-wavelength studies have revealed crucial information regarding the formation and evolution of these sources. While studying the optical counterparts of these sources it was found that nearly 20-70 percent of the LMXBs detected in the nearby Universe reside in globular clusters (Angelini et al., 2001; Minniti et al., 2004; Jordán et al., 2004; Clark, 1975).

1.3.1 Globular cluster X-ray sources

Globular clusters are known to be a collection of stars which are tightly bound by gravity and believed to host stars of nearly the same origin and formation mechanisms. These are highly dense systems with mainly old stellar population. The cores of these globular clusters seem to favour the formation of LMXBs as suggested by an observed correlation between the stellar interaction rate and the presence of LMXBs (Clark, 1975; Verbunt & Hut, 1987; Bellazzini et al., 1995; Barmby et al., 2007; Peacock et al., 2009). Since LMXBs are also found in the field of a galaxy where stellar densities are typically low, the formation of field LMXBs is also proposed to be from globular clusters. According to the theory, the field LMXBs might have originated inside a globular cluster and later got ejected from it (Kundu et al., 2002). Also, the possibility for an in-situ formation of field LMXBs had been proposed by Maccarone et al. (2003).

The preferential association of LMXBs to globular clusters is a widely studied yet interesting topic as it presents multiple dimensions to probe into the dynamics of the system. Globular clusters are regarded as simple stellar population (SSP) with well defined parameters such as age and metallicity and these information can be crucial in understanding the evolution of LMXBs. Kim et al. (2006) confirmed that the probability to find LMXBs in red globular clusters is nearly three times higher than in blue globular clusters. Also, they find that the probability of harboring an LMXB is higher near the galaxy centres compared to outskirts. Also, Kundu et al. (2007) proposed that some of the brightest metal rich red globular clusters might be hosting multiple LMXBs. Further, they suggest the possibility that the field LMXBs are formed in situ as they are more concentrated. Sivakoff et al. (2007) put forward

a size dependence of LMXB evolution, the compact systems being more likely to host an LMXB.

In 2008, using a sample of 24 early-type galaxies, Humphrey and Buote analysed the X-ray luminosity function (XLF) of each galaxy (Humphrey & Buote, 2008). According to this study, the spatial distribution and specific frequency of LMXB population is similar to that of globular clusters confirming the results of previous studies that all LMXBs form in globular clusters. Paolillo et al. (2011) while studying LMXB population in NGC 1399, again found evidences to support in situ formation of field LMXBs. They also suggested that the LMXB formation likelihood can be affected independently by metallicity, mass and structural parameters of their host globular clusters. Further, it is proposed that globular cluster LMXBs are slightly brighter than field LMXBs. Studies have also been carried out on the optical variability of the X-ray point sources and observed a relationship between X-ray and optical variabilities (Shih et al., 2011; Jithesh et al., 2014). Current studies on these sources focus on resolving their optical counterparts and also seek the help of multi-wavelength observations. Among the bright X-ray sources, a class of objects known as ultra-luminous X-ray sources have attracted attention as described below.

1.3.2 Ultra luminous X-ray sources

Ultra luminous X-ray sources (ULXs) are non-nuclear X-ray sources in nearby galaxies with luminosities above the Eddington limit ($\approx 2 \times 10^{39}$ erg/s for a 10 $M_{\odot}$ black hole). It is also possible that ULXs consist of stellar mass black holes accreting at super Eddington rates (Fabbiano, 1989; Mukai et al., 2003). Also, it is proposed that these systems contain intermediate mass black holes with standard accretion disks (Colbert & Mushotzky, 1999). ULXs were first discovered by Einstein observatory (Long et al., 1981) while subsequent telescopes such as ROSAT and ASCA studied them extensively (Roberts & Warwick, 2000). However, the advent of *Chandra* X-ray Observatory with its high resolution images triggered crucial developments in this field.

Super Eddington accretion rates coupled with the possibility of anisotropic emission can account for ULXs being black hole X-ray binaries (King et al., 2001, BHXBs). The ULXs might be representing the high luminosity tail of a galaxy's

normal BHXB population (Gilfanov, 2004). Thus, studying the population of ULXs might prove beneficial in characterising the kind of BHXBs residing in them. There can be high mass X-ray binaries (HMXBs) normally found in actively star forming galaxies or LMXBs generally found in ellipticals (Angelini et al., 2001).

ETGs contain only nearly one third of the known ULX population (Feng & Soria, 2011). This cannot be attributed entirely to an observational artefact as the local Universe is known to contain more late-type galaxies compared to ETGs. Specific frequency of ULXs in early-type galaxies is reported to be around ten times smaller than their late-type counterparts (Swartz et al., 2011). Also, the ULXs in ellipticals are seen to be less luminous than the ones in late-type galaxies (Irwin et al., 2004). This also explains why ULXs residing in late-type galaxies are well studied. As a result, the ULX population in nearby ETGs remain to be well understood and these need to be explored further. In most of the cases, the optical emission associated with the X-ray sources represent the integrated light from a globular cluster hosting them. Even the highest resolution which can be achieved by instruments in use currently is not sufficient to resolve the companion star of the binary systems which produces the X-rays. In this light, we carry out a stellar population synthesis of the star clusters hosting X-ray point sources to study more about the dynamics of these systems. The technique of stellar population synthesis is briefly introduced in the next section

1.3.3 Stellar population synthesis (SPS)

The integrated light from a galaxy might be enclosing crucial information about the star formation history of the galaxy. The earliest methods to model the integrated light from galaxies were based on trial and error analyses (Faber, 1972; Pickles, 1985). These were succeeded by a method known as evolutionary population synthesis (Tinsley, 1978; Bruzual A. & Charlot, 1993; Vazdekis, 1999). The main parameters employed in this technique are star formation history (SFR), initial mass function (IMF) and the extent of chemical enrichment of the galaxy. Assuming the time evolution of these parameters, the age dependent evolution of stars in the Hertzsprung- Russel (HR) diagram is computed. This gives the integrated spectral evolution of the underlying stellar population.

A serious drawback of the SPS models is their large uncertainties. Some poorly understood phases of the stellar evolution such as the asymptotic giant branch (AGB) can introduce tremendous uncertainties as these phases influence the integrated light (Charlot et al., 1996; Yi, 2003). Age and metallicity might affect the light in the same way giving rise to age-metallicity degeneracy (Worthey et al., 1994). However, the method when coupled with refined spectral diagnostics taking account of invidual stellar absorption line features can overcome this limitation (Jones & Worthey, 1995).

Two main ingredients of SPS models are stellar evolution prescription and stellar spectral library. Le Borgne et al. (2003) compiled a group of observed spectra of stars with wide range of metallicities named as 'STELIB'. Bruzual & Charlot (2003) is one of the most popular and widely used SPS models. This model uses 'STELIB' which allows the interpretation of integrated spectra of star clusters in the wavelength range 3200 - 9500 Å. The model reproduces the optical and near infra-red colour magnitude diagrams of Galactic star clusters of various ages and metallicities.

Motivated by the result that the photometric properties of the Bruzual & Charlot (2003) model match well with the observations of nearby star clusters, we attempt a population study of optical counterparts of X-ray point sources in nearby galaxies. We summarise this work in Chapter 2.

Apart from the globular cluster X-ray sources, another important constituent of the X-ray emitting population in nearby galaxies is the central super massive black hole. Hence, we extended our work to include a photometric study on the central regions of nearby galaxies which is introduced in the next section.

1.4 Study of central light concentration in nearby galaxies

In this work, we explore the possible connections between the central intensity ratio (CIR) in nearby galaxies and the super massive black holes residing in their central regions. We also explore the relationship between the CIR and the properties of the SMBH host galaxies. In order to understand the significance of this work, some prior knowledge about the co-evolution of SMBHs and their host galaxies is required.

Since our sample consists of galaxies with classical and pseudo bulges, a short note on how these bulges can be distinguished is also provided.

1.4.1 Co-evolution of SMBHs and their host galaxies

SMBHs residing at the centres of many ETGs and bulges in the nearby Universe are believed to be intimately connected with the evolution of their host galaxies (Kormendy & Richstone, 1995; Marconi & Hunt, 2003; Ho, 1999). Kormendy & Richstone (1995) is among the first who reported correlations between SMBHs and their host galaxies. Using a sample of eight galaxies with known dynamical masses, they reported that the masses correlate with the blue band luminosities of bulges of spirals and ellipticals. As more and more black hole masses began to be known, this relation has evolved over the years (see review by Kormendy & Ho 2013). Another milestone in this field was the discovery of the correlation between SMBH masses and the central velocity dispersion of galaxies simultaneously by two groups (Ferrarese & Merritt, 2000; Gebhardt et al., 2000). These kinds of correlations are generally known as scaling relations. Owing to the exploration of these relations by several authors, it was known that the spirals and ellipticals may not follow the same relations (Kormendy & Kennicutt, 2004). Further, Hu (2008) suggested that these relations also differ in the case of classical and pseudo bulges classified using the criteria of Kormendy & Kennicutt (2004). Various scaling relations observed differently by pseudo and classical bulges are extensively discussed in Kormendy & Ho (2013). Before explaining how pseudo bulges and classical bulges seem to differ in the case of scaling relations, a short introduction about how to morphologically distinguish them is necessary.

1.4.2 Classical and pseudo bulges

Elliptical galaxies and massive bulges in disc galaxies are morphologically similar. These systems also satisfy the same fundamental and photometric plane correlations (Kormendy, Fisher & Droy 2010). Initially all buges were thought to be classical in nature as they were believed to be formed as a result of mergers similar to elliptical galaxies. Some authors found that at least some of the bulges, believed earlier to be classical, are more disk-like. These may also be formed due to slow and secular

evolution. These might also have undergone minor mergers but their evolution is rather slow and isolated (Kormendy & Kennicutt, 2004; Kormendy & Bender, 2012). Some of the observational criteria used to distinguish between classical and pseudo bulges are listed below

1. Pseudo bulges have disky morphology. They might contain spiral structures all the way down to their centres. Classical bulges are rounder than their discs and cannot have spiral structures.

2. The presence of a nuclear bar indicates that a pseudo bulge dominates the central light.

3. In edge-on galaxies, the identification of boxy bulges indicates the presence of pseudo bulge. These might be representing edge-on bars.

4. Most of the pseudo bulges have Sérsic index, $n \leq 2$ whereas classical bulges have $n > 2$.

If the classification is based on many criteria, it is considered as more robust. The two bulges are thought to be significantly different in their evolutionary histories which might be reflecting in their scaling relations with the central SMBH.

After the study of Hu (2008), this was later indirectly supported by Graham (2008) as he found a difference in the case of barred galaxies and unbarred disc galaxies. Kormendy et al. (2011) reported that black hole masses do not correlate with either the luminosities or the velocity dispersion of their host pseudo bulges. Apart from pseudo bulges, black hole masses were also not found to correlate with the properties of galaxy discs (Kormendy & Gebhardt, 2001).

The relationship of SMBHs with their host galaxies is an actively pursued research problem. As more and more dynamical mass measurements of SMBHs are being reported every day, updated studies are significant in this field. Hence we attempted a photometric study at the centre of nearby galaxies motivated by SMBH-host galaxy scaling relations. This work is summarised in Chapter 3.

1.5 Co-evolution of nuclear rings, bars and the central intensity ratio of their host galaxies

The central region of barred galaxies is believed to enclose crucial morphological information on different components of the galaxies such as nuclear rings, bars and spiral arms. *HST* made it possible to resolve the central regions of disc galaxies and hence helped in analysing their central morphology and kinematics. Such studies pointed out that many of the galaxies evolved secularly out of their discs. This kind of dynamical evolution is known as secular evolution.

1.5.1 Role of bars in secular evolution

In any rotationally supported system, deviation from axial symmetry promotes angular momentum transfer due to gravitational torques. This re-distribution of angular momentum is believed to be carried out most efficiently by means of stellar bars (Weinberg, 1985; Athanassoula, 2002). Bars play a significant role in driving gas from outer regions of the disc to the inner regions thereby triggering secular evolution (Kormendy, 1982; Hunt & Malkan, 1999; Knapen et al., 2002; Kormendy & Kennicutt, 2004). Figure 1.3 shows a typically barred spiral galaxy NGC 4394. Bar driven evolution of disc galaxies can only be understood by studying the dynamical evolution of the bar. In any rotating disc, the mean position of a star is fixed and it executes radial oscillations around its mean position. The presence of a bar can exert gravitational pull on the star causing large perturbations in its orbit. When the angular velocity of the bar matches with the radial oscillations of the star, resonances are formed. These are known as inner Lindblad resonances (ILRs). In regions near resonances, gas clouds collide and result in dissipation. Hence, the density in this region increases and triggers star formation (Athanassoula, 1994; Buta & Combes, 1996).

1.5.2 Formation of nuclear rings

Nuclear rings or circum-nuclear starburst rings (CNRs) are mostly found in barred galaxies (Knapen et al., 1999; Laurikainen et al., 2004). The nuclear ring residing in

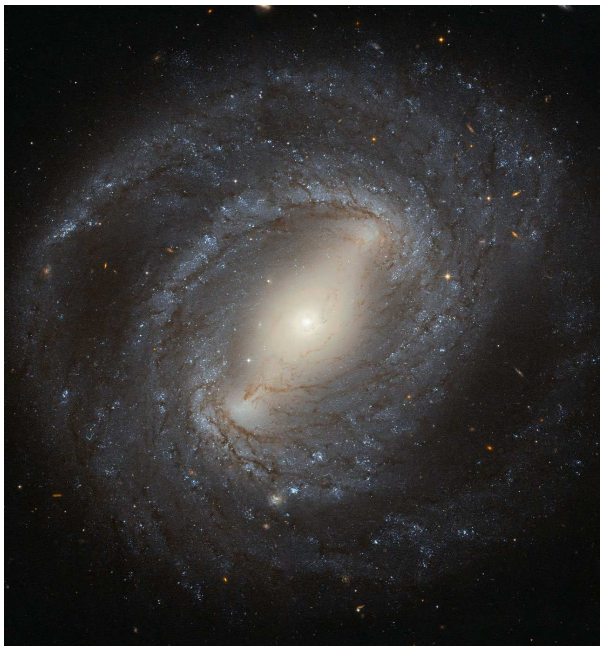

Figure 1.3: *HST* image of barred spiral galaxy NGC 4394. Image Courtesy: **www.nasa.gov**

NGC 1512 is shown in Figure 1.4 as an example of typical nuclear rings in galaxies. The dynamical evolution of the bar is believed to result in the formation of nuclear rings (Kormendy & Kennicutt, 2004). In the case of nuclear rings found in unbarred galaxies, merger events and other non-axisymmetric features like strong spiral arms might be forming these rings (de Zeeuw et al., 2002). The origin of nuclear rings is believed to be the gravitational torque from the non-axisymmetric bar potential causing gas infall towards the galaxy centres (Athanassoula, 1994). During this process, the inflow of gas slows down near the vicinity of ILRs. This results in the accumulation of gas leading to the formation of rings (Buta & Combes, 1996).

Though there are a number of observational and theoretical studies that try to explain this coupled evolution of rings and bars, the role of nuclear rings in the evolution of their host galaxies is not clearly understood. In fact, there are few studies reporting direct correlations of properties of bars and nuclear rings with their host galaxies.

In the final part of our work, we study the co-evolution of nuclear rings, bars and the central intensity ratio of their host galaxies. This is an ongoing research field as new simulations are being reported. Our work on a sample of 14 spiral galaxies

Figure 1.4: *HST* image of nuclear ring in the galaxy NGC 1512. Image Courtesy: **www.apod.nasa.gov**

hosting nuclear rings is summarised in Chapter 4.

The entire work presented in this thesis is carried out using the photometric images captured by Hubble Space Telescope. Hence, we give a brief introduction about Hubble Space Telescope and its associated instruments in the following section.

1.6 Hubble Space Telescope

Hubble Space Telescope (HST) named after the famous american astronomer Edwin. P. Hubble was launched in April, 1990. The *HST* was originally built by National Aeronautics and Space Administration (NASA) of the United States. European Space Agency (ESA) joined this project later and currently the *HST* is jointly operated by NASA and ESA. Hubble's targets are selected by Space Telescope Science Institute (STScI). The *HST* is a unique telescope as it can be serviced on orbit by space shuttle astronauts. Since its launch in 1990, five service missions were carried out so far. The *HST* is expected to be in operation at least till 2030. The *HST* as photographed on its fifth servicing mission in 2009 is shown in Figure 1.5

Initially when it was launched, the *HST* carried five instruments designed to make observations in the near infra-red, visible and ultraviolet regions of the electromagnetic spectrum: the Wide Field and Planetary Camera (WF/PC), High Speed Photometer (HSP), Faint Object Spectrograph (FOS), Goddard High Resolution Spectrograph (GHRS) and the Faint Object Camera (FOC).

We used the images taken by two *HST* instruments in our analysis. A short

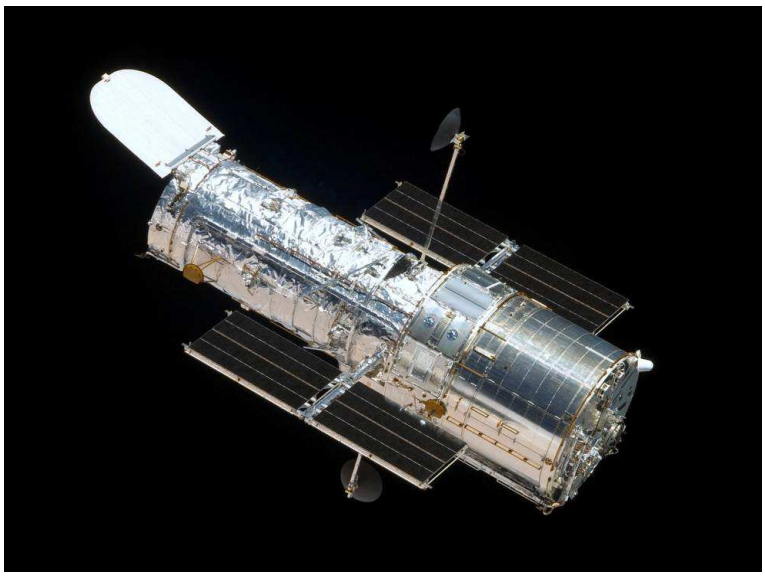

Figure 1.5: The *HST* as photographed on its fifth servicing mission in 2009. Image Courtesy: **www.nasa.gov**

description about each of them is given below.

1.6.1 Wide Field Planetary Camera 2 (WFPC2)

This instrument was installed in *HST* in 1993 by servicing mission 1. Currently this is not on board as it was removed and replaced by Wide Field Camera 3 (WFC3) in 2009.

The CCDs in WFPC2 were originally designed to detect radiations in the wavelength region 120-1000 nm. There were four identical CCD detectors and three of them were arranged in an L-shaped structure termed as Wide Field Camera (WFC). The fourth CCD served as the Planetary Camera (PC). WFC and PC images are combined to produce the final image. WFPC2 was Hubble's main camera until the installation of Advanced Camera for Surveys in 2002.

1.6.2 Advanced Camera for Surveys (ACS)

The ACS, as the name suggests, is specifically designed to map large areas of sky with very high resolution. This was installed in *HST* by mission 3B as a replacement of FOC. ACS images display remarkably sharp image quality. It has a wide field

of view and enhanced sensitivity. The ACS observes radiations from visible to near infra-red regions of the electromagnetic spectrum. ACS consists of three cameras: the wide field camera, the solar blind camera and the high resolution camera. Each of these performs a different function. Ever since its launch in 2002, the ACS has provided major breakthroughs in Astronomy.

We used publicly available images of these instruments from Mikulsky archive for space telescopes (MAST). These images were analysed with the help of a number of softwares. We used mainly three softwares for data analysis in the present work. Each of these are listed below along with their uses.

1.7 Softwares used in data reduction

1.7.1 Image Reduction and Analysis Facility (IRAF)

IRAF stands for the image reduction and analysis facility which is a general purpose software system created for the purpose of reduction and analysis of astronomical data. *IRAF* can be used for photometric as well as spectroscopic data reduction. This software was written at the National Optical Astronomy Observatory (NOAO) situated in Tucson, Arizona. It is basically designed for Unix based systems but it can also be used in Microsoft Windows with some modifications.

Various packages are available in *IRAF* for data reduction. User can also add external packages. In particular, *STSDAS* and *TABLES* packages provided by *STScI* are of great use in photometry. Each package consists of a number of tasks using which image reduction can be performed. *IRAF* can be used to calibrate the fluxes and positions of astronomical objects. It can also be used to calculate redshifts by analysing absorption and emission lines of a spectrum.

We used *IRAF* for finding the optical counterparts of bright X-ray point sources in our sample galaxies. This was done with the help of 'ellipse' and 'apphot' tasks in *IRAF*.

1.7.2 Source Extractor (SExtractor)

SExtractor was developed by E. Bertin and S. Arnouts in 1995. SExtractor is a program that builds a catalogue of objects from an astronomical image and it can be used to perform their photometry. It can perform photometry on both scanned photographic plate data and CCD. SExtractor has the capacity to handle large files in fits format and it offers very high speed. The user can control input parameters and choose the output parameters to be displayed.

The second part of our work deals with the central regions of early-type galaxies. This work is based on the central light concentration which is obtained with the help of SExtractor. We used it to identify the centres of galaxies and perform photometry in two specific apertures.

1.7.3 GALAXEV

GALAXEV is a tool to study galaxy evolution. The code *GALAXEV* makes use of isochrone methods of Bruzual and Charlot (2003) and it serves as a library of evolutionary population synthesis models. *GALAXEV* allows the computation of spectro-photometric evolution of stellar populations with various ages and metallicities at a resolution of 3 Å across the range of wavelengths 3200- 9500 Å. The default distribution of the code consists of 26 stellar population synthesis models constructed using the Padova 1994 evolutionary tracks. *GALAXEV* contains models using two initial mass functions: Chabrier (2003) and Salpeter (1955) with lower and upper mass cut-offs 0.1 $M_{\odot}$ and 100 $M_{\odot}$, respectively.

Chapter 2

Study of optical counterparts of bright X-ray sources in early-type galaxies

2.1 Introduction

The evolutionary history of galaxies is believed to be embedded in their star clusters. Studying such stellar population might be a useful tool capable of unfolding the formation and evolution scenario of the whole galaxy. The easiest way to tap the information hidden in these point sources is to analyse their integrated magnitudes in multiple filters. Unresolved star clusters hosting X-ray sources are still more interesting class of objects as they provide another dimension to probe into the dynamics of the system.

Over the years, several studies were performed on the nature of X-ray point sources in nearby galaxies with an aim to unveil the formation mechanisms of the X-ray emitting sources. Significant studies on the X-ray emission of normal galaxies date back to 1989 with the help of Einstein X-ray observatory (Giacconi et al., 1979). Many such sources were found to be low mass X-ray binaries (LMXBs) residing in globular clusters. Systematic studies on globular cluster systems are expected to provide deeper insights into the star formation history and chemical enrichment of

galaxies (Ashman & Zepf, 1998; Harris et al., 2001). Though these are believed to be formed during the initial stages of galaxy evolution, these are also found in systems that had undergone subsequent star formation episodes. Thus, many of the early-type galaxies in the nearby Universe contain globular clusters exhibiting bimodal colour distribution (Gebhardt & Kissler-Patig, 1999; Larsen et al., 2001; Kundu & Whitmore, 2001). This bimodality might have resulted from the metallicity difference between the two kinds of population residing in them (Brodie & Strader, 2006).

Grindlay et al. (1984) suggested that all LMXBs in galaxies originated in globular clusters. High resolution X-ray observations by *Chandra* revealed that around 30-70 percent of the entire LMXB population reside in globular clusters. Further, the LMXBs preferentially reside in red globular clusters compared to the blue globular clusters (Fabbiano, 2006). In Milky Way and M31, it was found that metal rich globular clusters are more likely to host LMXBs (Bellazzini et al., 1995). Further studies confirmed that the fraction of metal rich globular clusters hosting LMXBs are at least three times greater than that of metal poor clusters (Kundu et al., 2002; Kim et al., 2006; Sivakoff et al., 2007; Paolillo et al., 2011). This effect can either be attributed to age or metallicity. Kundu et al. (2003) suggested the metallicity to be the main factor as they could not find any correlation between the age of the clusters and LMXB parameters. Maccarone et al. (2004) proposed that irradiation induced winds in metal poor clusters accelerate their evolution resulting in the formation of smaller number of globular clusters compared to the metal rich clusters. Such strong winds in metal poor clusters may be attributed to their less efficient line cooling in comparison with metal rich clusters (Iben et al., 1997).

The simplest parameter used to describe a globular cluster is its specific frequency which is defined as the number of clusters per unit galaxy luminosity (Harris et al., 1991). Several studies revealed a second order correlation between the integrated luminosities of LMXBs in a galaxy and globular cluster specific frequency (Kim et al., 2006). This might be implying an underlying relation between globular cluster metallicity and LMXB formation. Various theories have been put forth on LMXB formation including different stellar sizes and IMFs (Bellazzini et al., 1995). Some authors suggested that globular clusters found near the centres of galaxies possess compact cores and high central densities so as to withstand tidal disruption

leading to dynamical LMXB formation (Kim et al., 2006). It was also speculated that metallicity dependent magnetic breaking (Ivanova et al., 2005) can also play a key role in LMXB formation. None of these theories are observationally confirmed.

Though most of the LMXBs reside in globular clusters, native field binaries are also detected (Maccarone et al., 2003; Irwin, 2005; Juett, 2005; Kim et al., 2006). LMXBs in the field can act as a good proxy of the stellar mass of their host galaxies (Gilfanov, 2004). It was also found that the number of sources per unit stellar mass is very high in younger galaxies (Zhang et al., 2012). Field LMXBs were also suggested to be formed in globular clusters and ejected later due to formation kicks or evaporation of the parent cluster (Kundu et al., 2002). Also, there have been evidences to suggest that a considerable fraction of LMXBs in the field were originated in the field itself (Juett, 2005; Irwin, 2005). Since most of the subsequent studies failed to find a substantial difference between the LMXBs residing in globular clusters and those in field (Kim et al., 2006), their origin and formation processes are yet to be properly understood.

Apart from the LMXBs, the early-type galaxies also contain ultra-luminous X-ray sources (Kaaret et al., 2017). These are off-nuclear X-ray point sources and their X-ray luminosities are in between that of the X-ray binaries and active galactic nuclei (AGNs; 10^{39} - 10^{41} erg/s). These could well be representing intermediate mass black holes (IMBHs) which can bridge the gap between stellar mass black holes and super massive black holes at the galaxy centres. Such IMBHs may have resulted from the hierarchical merging in the early Universe (Madau & Rees, 2001). In young dense stellar clusters, core collapse can lead to IMBH formation (Miller & Hamilton, 2002). It is also possible that ULXs can be just stellar mass black holes accreting at super Eddington accretion rates (King et al., 2001) or powered by relativistic jets (Körding et al., 2002).

All in all, the LMXBs along with ULXs residing in early-type galaxies constitute an interesting class of objects carrying essential information regarding the formation mechanism of the galaxies. With an aim to check for optical to X-ray association in unresolved clusters in nearby galaxies, we analyse the bright X-ray point sources in three early-type galaxies: NGC 1399, NGC 4552 and NGC 4649. Over the years, extensive studies have been carried out on all the three galaxies. We attempt a more specific analysis primarily aimed at studying the dependence of the X-ray

point sources on the optical properties of their host clusters.

Various studies have revealed that the optical colour of stellar systems is primarily driven by two parameters: age and metallicity. Also, we see that the evolution of globular cluster LMXBs is heavily influenced by the cluster's metallicity. Therefore, in order to carry out a significant study, it is highly necessary to select a homogenously distributed age sample so as to differentiate between various metallicities. Old elliptical galaxies in Virgo and Fornax clusters are good candidates as their average stellar age was found to vary between 8 to 14 Gyr (Trager et al., 2000). Further, many of these galaxies contain about 5000 to 10000 globular clusters. In our sample, NGC 1399 belongs to Fornax cluster and the other two galaxies are part of Virgo cluster.

NGC 1399 is a prominent member of Fornax galaxy cluster and is the central giant elliptical (cD) galaxy of the cluster. The globular cluster system of NGC 1399 is probably the most studied object among the nearby galaxies as its specific frequency is around four times higher than its average in other ellipticals (Angelini et al., 2001; Kim et al., 2006). Also, it was found to exhibit colour-metallicity non linearity (Blakeslee et al., 2012). Spectroscopic studies show that it is located at a distance of about 20 Mpc from our galaxy (Dunn & Jerjen, 2006). While investigating the LMXB system in NGC 1399, Angelini et al. (2001) found that the most luminous X-ray sources reside in globular clusters. Further, Paolillo et al. (2011) confirmed that the red globular clusters residing near the galaxy cores contain a large fraction of LMXBs. ULXs detected in the galaxy were also found to be interesting objects and their nature was investigated (Devi et al., 2007; Jithesh et al., 2014).

NGC 4552 resides in Virgo cluster and it is situated at a distance of 17.1 Mpc (Xu et al., 2005). This galaxy is considered as an elliptical galaxy though some studies classify it as a lenticular galaxy (Cappellari et al., 1999). The galaxy with its compact core has a strong radio source (Filho et al., 2000). This is also believed to contain a central black hole possibly accreting matter via tidal stripping of a nearby star. Since the observed emission from the central region of this galaxy is of low luminosity, the source at the core is termed as a mini-AGN (Cappellari et al., 1999; Colbert & Mushotzky, 1999). Xu et al. (2005) carried out extensive studies on the LMXBs in this galaxy and detected three ULXs residing in it. They also identified that one of the ULXs resides in a globular cluster. Subsequent studies

on this galaxy were constrained as part of larger sample of galaxies (Sivakoff et al., 2007; Zhang et al., 2012) and the LMXBs in this galaxy seem to require further exploration.

The third member of the sample, NGC 4649 is another giant elliptical galaxy discovered in Virgo cluster. This galaxy has a spiral galaxy companion (NGC 4647) in close proximity with which the galaxy is believed to be interacting (Young et al., 2006). This galaxy contains a rich globular cluster system (Harris et al., 1991) and large number of LMXBs (Randall et al., 2004). Roberts et al. (2012) reported the discovery of a new variable ULX residing in a globular cluster in this galaxy. Several studies have been carried out to investigate the nature of LMXBs in NGC 4649 (Mineo et al., 2014; D'Abrusco et al., 2014). It was found that red globular clusters are more centrally concentrated compared to the blue ones (Brodie & Strader, 2006; D'Abrusco et al., 2014; Mineo et al., 2014). It was also speculated that many of the low luminosity sources are field LMXBs ejected from globular clusters (D'Abrusco et al., 2014). Recent studies on the LMXBs in this galaxy are mainly based on X-ray luminosity functions (Peacock & Zepf, 2016).

Though several studies performed in these galaxies were aimed at unveiling the dependence of X-ray point sources on the optical properties of their hosts, there is still scope for a stellar population synthesis (SPS) of these sources. Such an approach is expected to provide significant information about various dynamical properties of the system such as star formation history, ages and stellar masses. SPS is an effective tool in tapping the information hidden in the spectral energy distributions (SEDs) of unresolved star clusters. In the present study, we carry out SPS analysis of X-ray point sources in NGC 1399.

2.2 The data

The main goal of our work is to study the nature of optical counterparts of X-ray point sources in early-type galaxies and investigate their X-ray to optical association. Though we have numerous *Chandra* observations of X-ray point sources in nearby elliptical galaxies, most of them lack significant number of sources with X-ray counts greater than 60. In order to do two component X-ray spectral fitting using an absorbed power law and disk blackbody, it is required that the number of counts

Galaxy	Distance (Mpc)	N_X
(1)	(2)	(3)
NGC 1399	18.3	36
NGC 4552	15.9	47
NGC 4649	16.6	49

Table 2.1: (1) Name of the galaxy; (2) Distance to the galaxy in units of Mpc as provided by Swartz et al. (2004); (3)Number of bright X-ray sources in the galaxy (N_X).

should be greater than 60. This automatically imposes a constraint on our sample selection. In addition, it could also happen that many of these sources have either no optical counterparts or they are outside the field of view of the *HST* instrument. We, therefore, required a sample of statistically significant number of bright X-ray sources with optical counterparts in at least two *HST* bands. Though significant information can be gathered from the photometric measurements in one band, it is always useful to compute the optical colour as it is an important parameter in stellar population models.

Using the base sample of 82 galaxies (Swartz et al., 2004), we searched for galaxies with deep *Chandra* observations that have corresponding *HST* images in *F475W* and *F850LP* filters. Devi et al. (2007) had analysed a sub sample of this where they attempted the spectral fitting with two components and derived luminosities in a more efficient method. We selected the galaxy NGC 1399 from this sample and adopted the values of X-ray luminosities. NGC 4649 and NGC 4552 were also included in this sample but the number of sources were not sufficient for our analysis. We, therefore, adopted the luminosities of the X-ray point sources in the galaxy NGC 4649 estimated using a recent *Chandra* observation (Jithesh, private communication). Xu et al. (2005) had carried out detailed X-ray analysis of 47 point sources in NGC 4552. Hence, we used the X-ray flux determinations from this paper. The final sample consists of 36 X-ray sources in NGC 1399, 49 sources in NGC 4649 and 47 sources in NGC 4552. The properties of the sample galaxies are listed in Table 2.1.

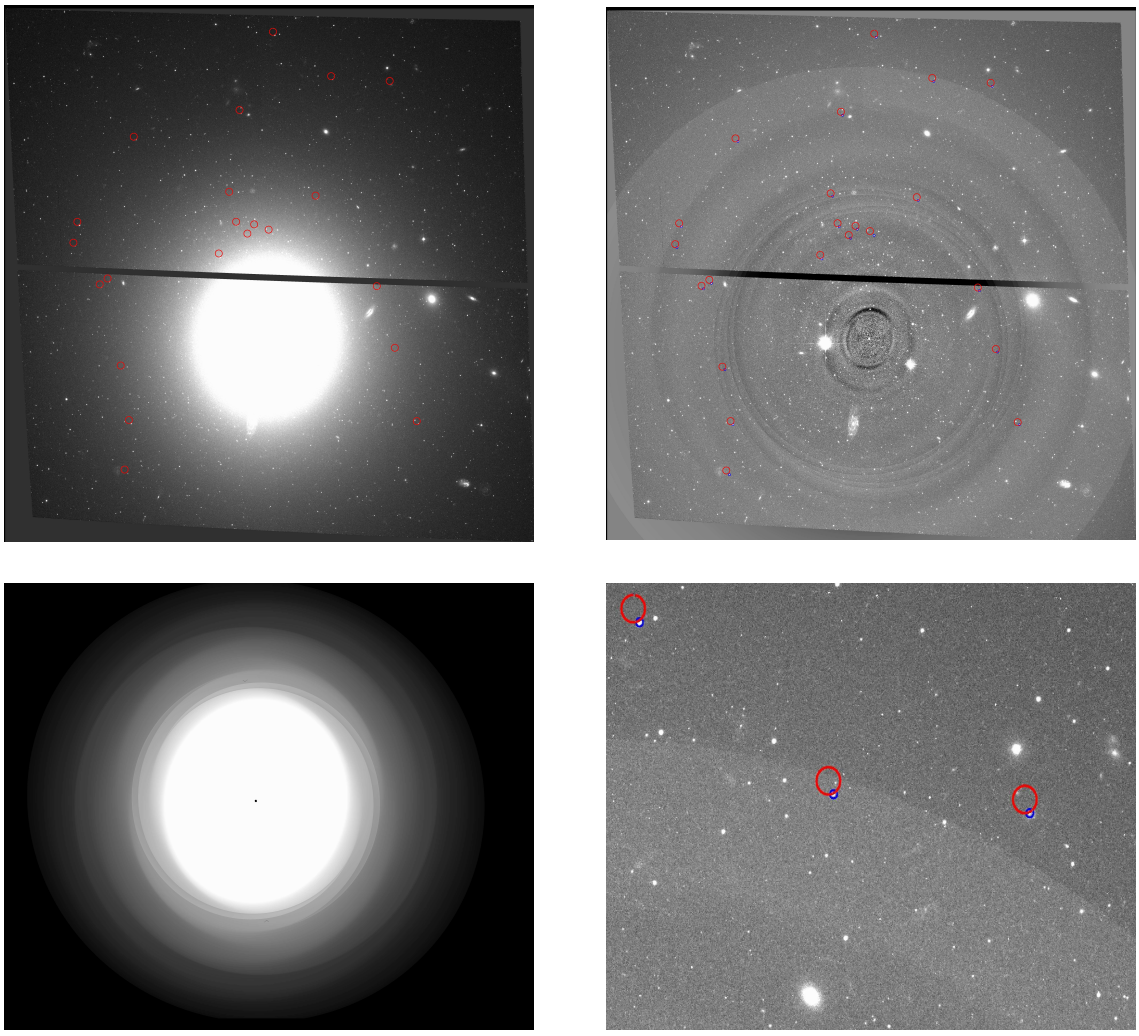

Figure 2.1: Images of the galaxy NGC 1399 (anti-clockwise from top left panel): (a) Galaxy image in *HST* band *F475W* (b) model of the galaxy obtained using *IRAF* (c) residual image obtained after subtracting the model from galaxy image and (d) a section of the galaxy in which the red circles denote the X-ray positions as identified by *Chandra* and blue circles denote optical sources identified as counterparts by *HST*

.

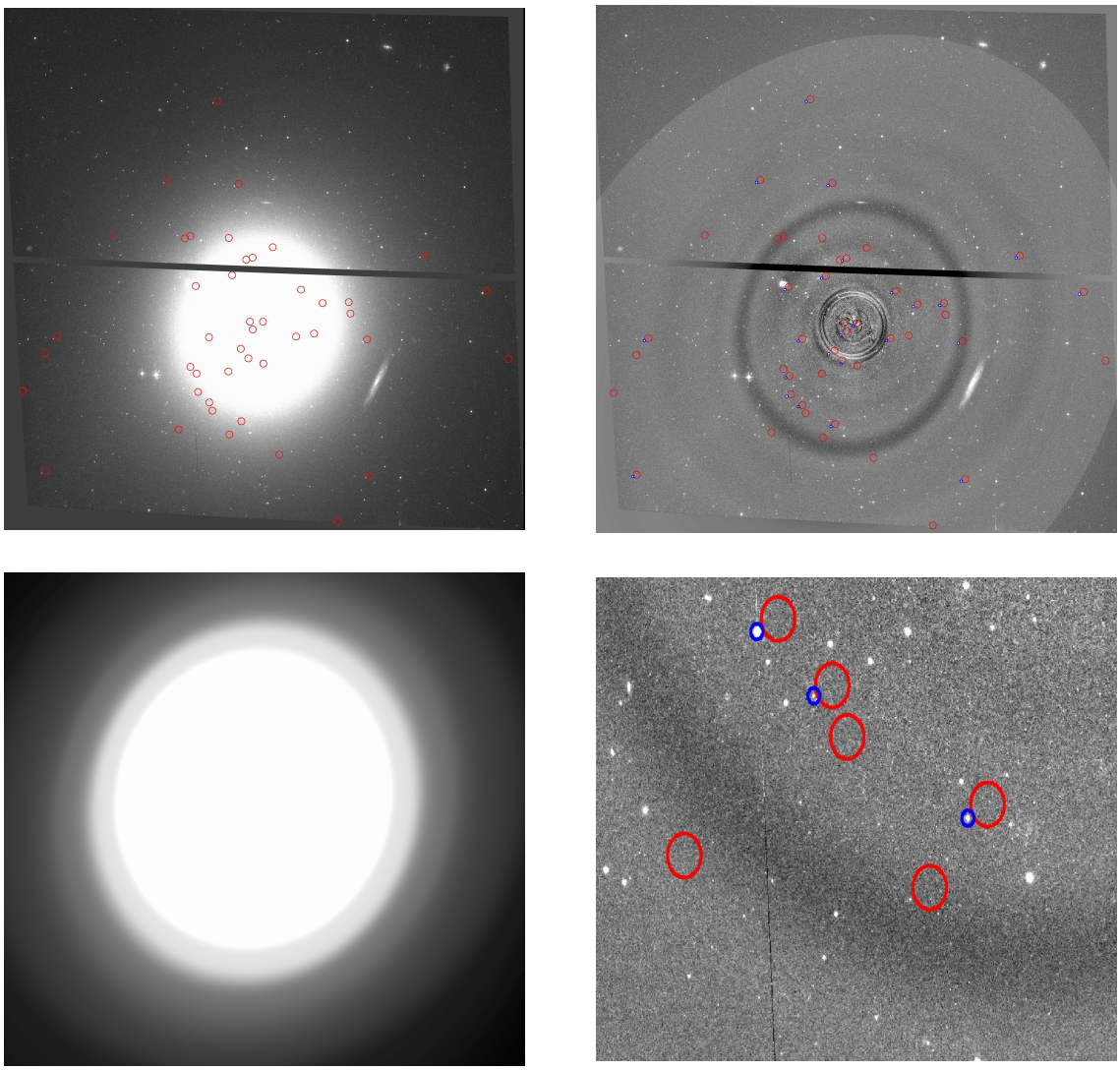

Figure 2.2: Images of the galaxy NGC 4552 (anti-clockwise from top left panel): (a) Galaxy image in *HST* band *F475W* (b) model of the galaxy obtained using *IRAF* (c) residual image obtained after subtracting the model from galaxy image and (d) a section of the galaxy in which the red circles denote the X-ray positions as identified by *Chandra* and blue circles denote optical sources identified as counterparts by *HST*

.

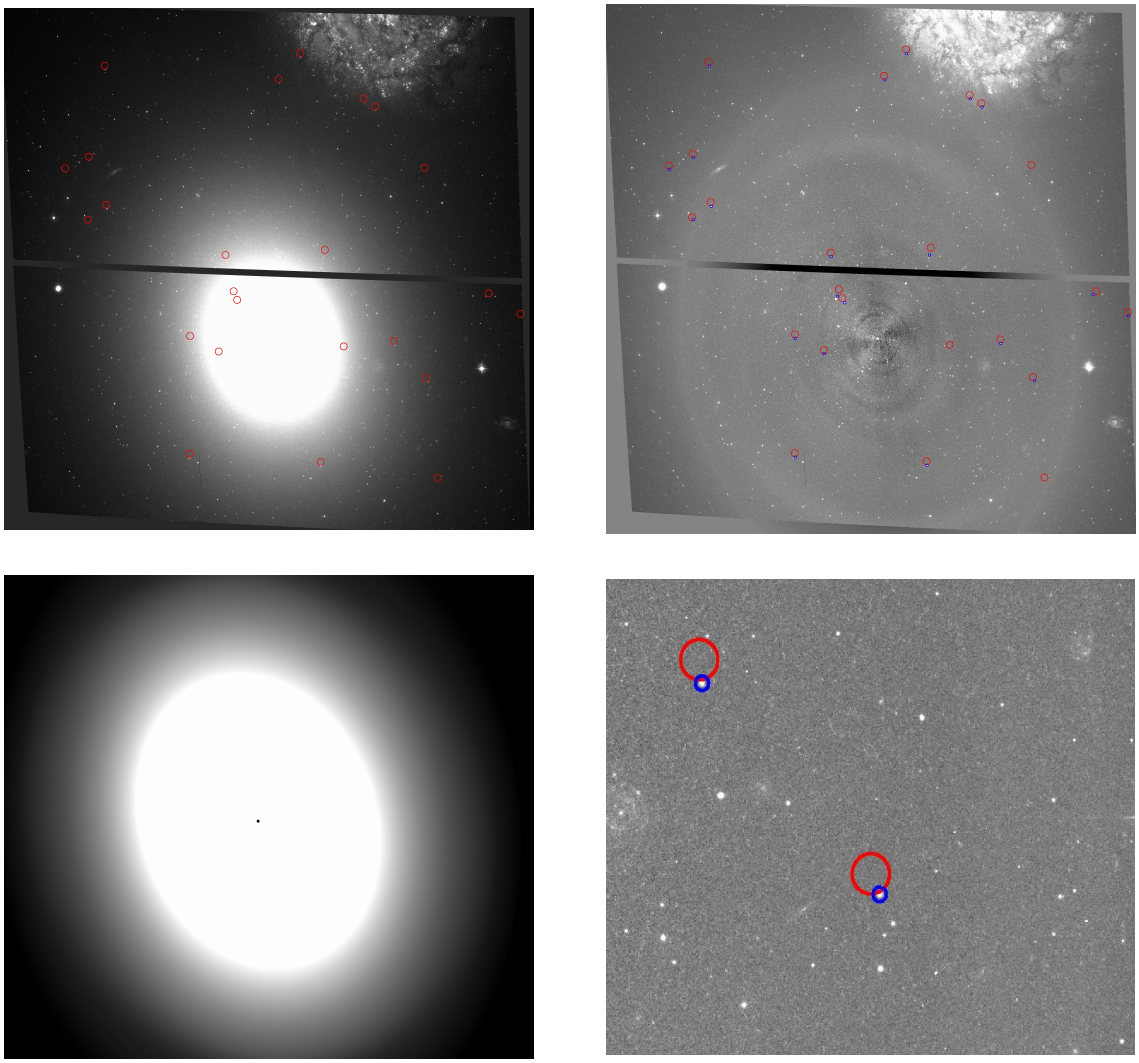

Figure 2.3: Images of the galaxy NGC 4649 (anti-clockwise from top left panel): (a) Galaxy image in *HST* band *F475W* (b) model of the galaxy obtained using *IRAF* (c) residual image obtained after subtracting the model from galaxy image and (d) a section of the galaxy in which the red circles denote the X-ray positions as identified by *Chandra* and blue circles denote optical sources identified as counterparts by *HST*

.

2.3 Data Analysis

2.3.1 Optical analysis

To optically identify the X-ray sources, we used archival images of Wide Field Planetary Camera (WFPC) of *HST*. We performed the photometric analysis of these sources in two different *HST* filters namely *F475W* and *F850LP* for all the three galaxies. In order to identify the underlying stellar populations, it was essential to subtract the light of the galaxy and obtain the residual image. We performed this task with the help of *IRAF/STSDAS/ellipse* package. Bad pixels and extended objects were masked out during the ellipse fitting.

As part of the astrometry, it was required to identify the optical sources in each filter. We used the software source extractor (SExtractor) with a threshold 3 sigma to identify the total optical sources in an image. The X-ray contours when over plotted on the *HST* images, show a definite systematic off-set in all filters. The two instruments (*Chandra* and *HST*) differ in their angular resolutions, *HST* being more accurate than *Chandra* with a resolution of 0.05 arcsecs compared to 1 arcsecs of *Chandra*. We calculated the off-set in each image and shifted the X-ray coordinates by applying a common shift. The coordinates thus obtained were compared with those given by the source extractor output to identify the optical sources. Once we shifted the coordinates, a strict matching criterion with a radius of 0.5 arcsec was applied to identify the optical sources. Although a more relaxed search radius might aid in obtaining more globular cluster LMXBs, the probability for spurious detection might also be higher. It might also result in an increased number of duplicated matches. The chance probability of making a false match within the radius 0.5 arcsecs is reported to be 0.5- 2 percent (Kim et al., 2013). In cases where multiple optical sources were found around the X-ray detection spot, the nearest optical source was selected to be the real counterpart.

2.3.2 Aperture photometry

Though the magnitudes in different bands are given by *SExtractor*, we performed aperture photometry using *IRAF* for better accuracy. This was achieved by the task phot given by *IRAF* package *noao/digiphot*. We fixed the aperture value as

10 pixels. This task simply gives the net flux within a fixed radius from the center of the source. In NGC 1399, the photometric images were available in four optical bands (*F475W*, *F606W*, *F814W* and *F850LP*). We performed the analysis in all four bands. In *F606W* band, as we had to deal with three images covering different parts of the galaxy, we encountered a number of common sources. In such cases, the one with the highest flux was chosen as the magnitude of the counterpart.

2.3.3 Stellar population synthesis of the sources in NGC 1399

The stellar population synthesis code of Bruzual & Charlot (2003) was used for the analysis. The code computes the photometric and spectroscopic evolution of stellar population across the wavelength range 320-950 nm . The library *GALAXEV*, which is a part of the code, includes models for a wide range of ages and metallicities. The method of isochrone synthesis is used to compute the stellar spectral evolution in this code. Isochrones synthesis is based on the concept of simple stellar populations (SSPs). Isochrones specify the single age and single metallicity regions in the Hertzsprung-Russel (HR) diagram. SSPs are believed to be formed at around the same time and with the same initial elements. The evolution of such population is computed in the code based on stellar spectral libraries and theories of stellar evolution.

We computed the absolute magnitudes and broadband colours assuming a distance modulus of 31.46 as adopted from Devi et al. (2007). We adopted an average metallicity of 0.004 as reported by Ostrov et al. (1998). The Padova 1994 tracks were used for the analysis as recommended by the code. The Chabrier initial mass function (IMF) was used to generate the models. The code computes the evolution from ages 1×10^5 to 2×10^{10} years. The stellar population of NGC 1399 are believed to be relatively old as many of them are confirmed globular clusters. We used star formation rates of the order of 0.1 solar mass per year and early cut offs ($\approx$ 0.001 Gyrs).

Four magnitudes (*F475W*, *F606W*,*F814W* and *F850LP*) and three broadband colours ($F475W-F606W$, $F475W-F814W$ and $F475W-F850LP$) were extracted from the code. The magnitudes were converted to AB system to make it easier to

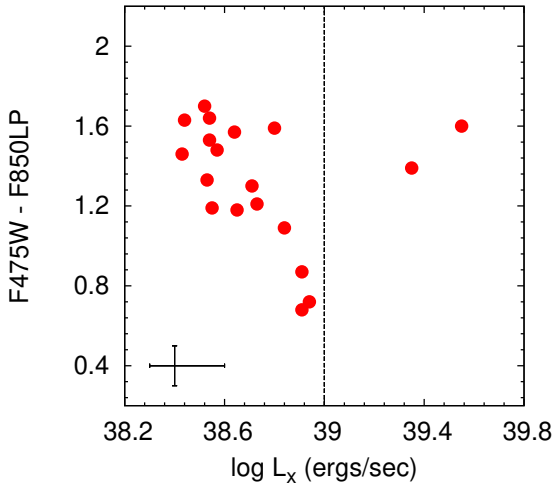

Figure 2.4: Plot of X-ray luminosities of bright X-ray sources Vs optical colour of their possible counterparts in the galaxy NGC 1399. The vertical line is drawn to denote the Eddington limit of X-ray luminosity for a 10 $M_\odot$ black hole. Typical error bars are shown in the lower left corner.

compare with the data. After extracting the models, the data were fitted with the model with the help of a minimisation algorithm. The masses and ages were found using the best fitting values of the model parameters.

2.4 Results

Out of the 36 sources in NGC 1399, 22 of the sources were found to be having genuine optical counterparts. We list the properties of these sources in Table 2.2. Figure 2.1(a) shows the original image of the galaxy NGC 1399 with the X-ray sources overplotted. The model image and the residual image obtained after subtracting the model from the original image are in Figure 2.1(b) and (c) respectively. The sources identified as the optical counterparts are also marked in Figure 2.1(d). Two ULXs were found to be having optical counterparts. We plot the log of the X-ray luminosities against the $F475W - F850LP$ colour of the sources as shown in Figure 2.4. We observe that the X-ray luminosities are anti-correlated with optical colours (rank correlation coefficient, r= 0.8 and the significance, $p >$ 99.99 percent).

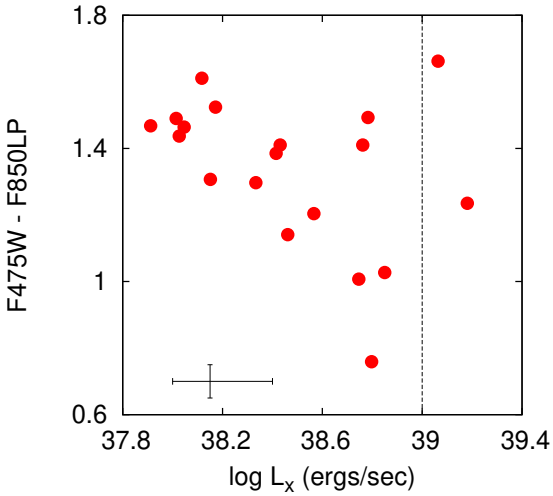

Figure 2.5: Plot of X-ray luminosities of bright X-ray sources Vs optical colour of their possible counterparts in the galaxy NGC 4552. The vertical line is drawn to denote the Eddington limit of X-ray luminosity for a 10 $M_{\odot}$ black hole. Typical error bars are shown in the lower left corner.

In galaxy NGC 4552, we had 47 X-ray sources selected from Xu et al. (2005) for which we identified 29 sources as optical counterparts as given in Table 2.3. One of these sources belonged to the central AGN and therefore we excluded it from our sample. Three other sources were too near to the centre making it difficult to clearly see the optical source. There were two extended sources seemingly background objects situated at the outskirts of the galaxy. Yet another source had two counterparts very close to each other. All these sources were excluded from the final analysis leaving 21 sources including two ULXs. The original image of NGC 4552 in *F475W* is shown Figure 2.2(a). The X-ray positions as observed by *Chandra* are marked. The model galaxy generated using *bmodel* task is shown in Figure 2.2(b). Also, Figure 2.2(c) shows the residual image and the identified optical counterparts can be seen in Figure 2.2(d). Here also, we observe a correlation coefficient of -0.86 with a significance greater than 99 percent as shown in Figure 2.5.

We find only 19 optical counterparts for a sample of 49 X-ray sources in NGC 4649 as shown in Table 2.4. Though there were three ULXs, none of them was found inside the *HST* field of view. The photometric image of the galaxy is shown

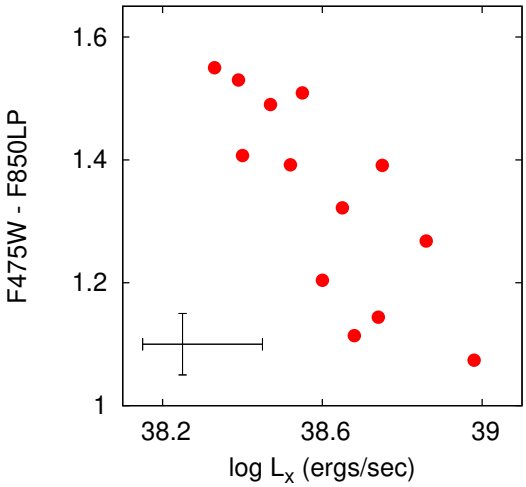

Figure 2.6: Plot of X-ray luminosities of bright X-ray sources Vs optical colour of their possible counterparts in the galaxy NGC 4649. The ULXs detected in this galaxy were outside the field of view of optical image used in this analysis. Typical error bars are shown in the lower left corner.

in Figure 2.3(a), model galaxy is shown in 2.3(b) and the residual image is shown in Figure 2.3(c). Here also we have excluded sources situated near the centre and the ones which seemed ambiguous on visual inspection finally reducing the number of counterparts to 13. Some of the counterparts are marked in Figure 2.3(d). This galaxy also shows a correlation between the X-ray luminosities and optical colours, the correlation coefficient being -0.83 with a significance over 99.99 percent as shown in Figure 2.6.

We obtained the ages and masses of all 22 sources by carrying out their SPS. The masses were found to be of the order of 10^5 solar masses as shown in Figure 2.7. The ages of these clusters were found to be lying in the range 10^7 to 10^{10} years as shown in Figure 2.8. Most of the clusters are old with ages nearer to or older than 10^{10} Gyrs. Stellar masses for five sources in our sample were previously determined by Humphrey & Buote (2008). Our results agree with their estimations with a slight deviation as expected as they have considered magnitudes in only two filters whereas our study involves four magnitudes.

We observed an anti-correlation between the stellar masses and X-ray lumi-

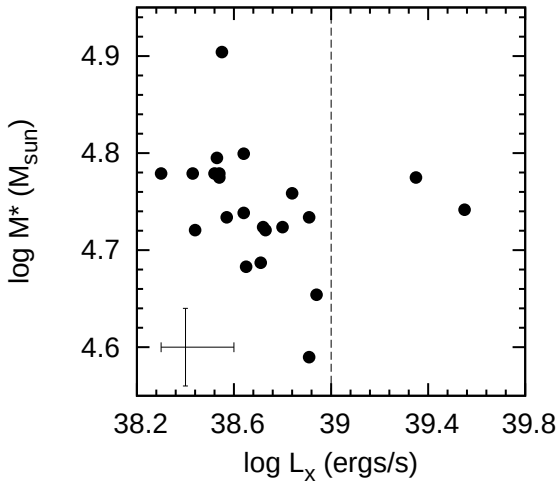

Figure 2.7: Plot of X-ray luminosities Vs the optical mass of the stellar clusters as computed by the code *GALAXEV*. The Padova 1994 tracks were used with Chabrier initial mass function.

nosities as shown in Figure 2.7. Excepting the two ULXs and an outlier with the heighest mass, the Spearman's rank correlation is found to be -0.62 with significance greater than 99 percent. Also, we observe that brighter X-ray sources are younger sources as seen in Figure 2.8. It is to be noted that the two ULXs included in the study are not following both the relations.

2.5 Discussion and Conclusion

We analysed the nature of optical counterparts of bright X-ray sources in three nearby elliptical galaxies: NGC 1399, NGC 4552 and NGC 4649. Archival *HST* images in two filters (*F475W* and *F850LP*) were used for the analysis. We find a strong correlation between X-ray luminosities and $F475W - F850LP$ colours with a very high significance in all the three galaxies. Though various studies were conducted in the past on the optical counterparts of X-ray point sources in nearby early-type galaxies, such a strong correlation was not reported. Further, we perform population synthesis on the counterparts of X-ray sources in NGC 1399 using magnitudes

in four filters and associated colours. We find that the less luminous the sources in X-ray, the more massive they are. We also observe that the sources with low X-ray luminosities are in general older.

There have been many significant discoveries in the past hinting an association between X-ray sources and their host stellar clusters. It is an established result that red globular clusters are more likely to host LMXBs than blue globular clusters (Fabbiano, 2006). Also we know that colour is closely related to metallicity. In Milky Way and M31, it was found that metal rich globular clusters are more likely to host LMXBs (Bellazzini et al., 1995). Angelini et al. (2001) reported a weak correlation between X-ray luminosities and $g - z$ colours in NGC 1399. They reported that the redder globular clusters are fainter X-ray sources which is consistent with our result. In their study, the LMXBs in NGC 1399 were divided into three groups: the first class consisted of X-ray sources with luminosities greater than 10^{39} erg/s, the second class of X-ray sources with luminosities in the range 2-10 $\times$ 10^{38} erg/s and the final class with low X-ray luminosities ($< 2 \times 10^{38}$ erg/s). It was reported that the weak correlation between X-ray luminosities and $g - z$ colours breaks down for the brightest sources. This is also consistent with our findings. In fact, we find the sources starting to deviate from the correlation towards the high luminosity ends with the ULXs completely defying it.

X-ray luminosity function (XLF) is a highly significant tool used to characterise the X-ray binary population in normal galaxies. The LMXB luminosity function is known to contain two remarkable breaks: a high luminosity break at $L_X \geq 2 \times 10^{38}$ erg/s (Gilfanov, 2004; Humphrey & Buote, 2008) and a low luminosity break at $L_X \approx 5 \times 10^{37}$ erg/s (Voss & Gilfanov, 2006; Kim & Fabbiano, 2010). These breaks may be attributed to differences in the type of the donor star in the X-ray binary or the evolutionary stage of the LMXB population. However, the XLF appears more or less smooth in the region between the two breaks. The observed correlation in this study is also found to be the strongest in this region.

Most of the optical counterparts of X-ray sources in these galaxies are confirmed globular clusters. The preferential association of LMXBs and red globular clusters is extensively explored in all the three galaxies of our sample (Angelini et al., 2001; Xu et al., 2005; Mineo et al., 2014). In the case of NGC 4649, the probable foreground extinction due to the disc of the nearby galaxy NGC 4697 was reported to be less

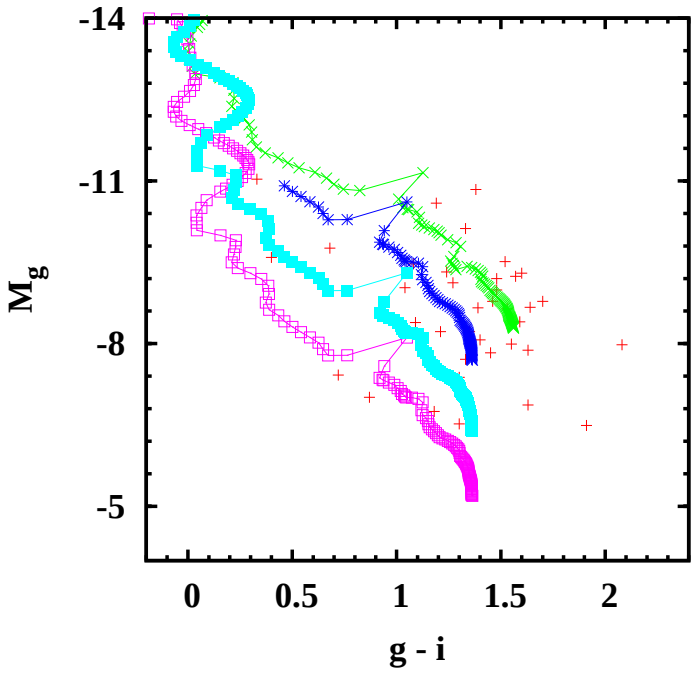

Figure 2.8: The colour magnitude diagram of the optical counterparts of X-ray sources in NGC 1399. The evolutionary tracks for different SFRs and initial cut-offs are shown. Each of the tracks contain regions of ages 10^7, 10^8,10^9 and 10^{10} Gyrs from top to bottom respectively. All tracks start with the initial mass of 10^3 $M_\odot$.

than 0.1 mag (Forbes et al., 2004). It was also confirmed that the number of ultra compact dwarfs associated with this galaxy is considerably small (Forbes et al., 2004). In nearby early-type galaxies, globular cluster systems are known to exhibit a bimodal colour distribution which might be indicating discrete globular cluster sub population (Kundu & Whitmore, 2001). Based on this bimodality, the division in red and blue globular clusters is located around $g - z$ = 1.1-1.2 (refer Peng et al. (2006) for Virgo cluster and Mieske et al. (2010) for Fornax cluster). Kim et al. (2013) report that the statistical significance of the metallicity dependence of LMXB formation is solid in the intermediate luminosity range (L_X = (0.2 - 5)$\times$ 10^{38} erg/s). The present correlation might well be a manifestation of this metallicity dependence.

Stellar population synthesis carried out on the optical counterparts of X-ray sources in NGC 1399 yielded significant information regarding these systems. We observe that the systems with lower X-ray luminosities are more massive compared to the ones having high luminosities. These massive clusters belong to the redder part of the bimodal distribution. It is already established that massive globular clusters are more likely to host LMXBs (Sarazin et al., 2000; Kim et al., 2006). This stems from the increased number of stars in massive clusters coupled with highly dense cores. This scenario naturally implies higher dynamical encounter rates in these clusters which promotes LMXB formation (Jordán et al., 2007). This is supported by the observation that when Milky Way globular clusters are binned by mass, the core-interaction rate is found to be linearly proportional to the stellar mass of the cluster (Smits et al., 2006). Further, the red globular clusters are mostly found near the galactic centres and these contain highly dense cores (Paolillo et al., 2011). Since LMXBs are preferentially associated with red globular clusters, the correlation in the present study is in agreement with these previous results.

Since age is the other ingredient which might be playing a crucial role in LMXB evolution apart from the metallicity of its host cluster, we have also explored this aspect. In fact, age determination is fairly reliable in the case of early-type galaxies and less likely to succumb to large systematic error as the single stellar population can be assumed in these galaxies. This difference is substantial when compared with an active and rejuvenated galaxy. In the former class of galaxies, most of the stars are old and less likely to be containing extremely young population (Serra &

Oosterloo, 2010). According to several spectroscopic studies, most of the globular clusters in early-type galaxies are older than 10 Gyr as shown by studies on NGC 1399 (Forbes et al., 2001) and for NGC 4649 (Pierce et al., 2006). Our result also supports this finding. Further, we see that massive globular clusters (with lower X-ray luminosities) are older than less massive ones (with higher X-ray luminosities). This suggests that younger clusters in the sample are more luminous X-ray sources. A similar observation was made by Zhang et al. (2012) in the case of galaxies. They report that the XLF of old galaxies is steeper than the young ones implying that younger galaxies contain more luminous LMXBs. Kim et al. (2006) and Fabbiano (2006) also reported the same.

Angelini et al. (2001) suggests the presence of multiple LMXBs per globular cluster which emit at the Eddigton rate to account for the highly luminous X-ray sources. Alternately, these systems may contain a large number of lower luminosity systems with high encounter rates compared to Galactic clusters. The second argument cannot be supported by our results as we observe highly luminous sources reside in blue globular clusters which are known to have lower encounter rates compared to red clusters (Fabbiano, 2006). Also, most of these globular cluster LMXBs exhibit variabilities both in their X-ray and optical luminosities (Jithesh et al., 2014). The correlations presented in this work appear despite such variability. This supports the possibility of multiple X-ray sources in these clusters (as optical counterparts are most likely globular clusters) so that the impact of variability is negligible for the entire cluster. In fact, the presence of 5-100 stellar mass black holes were predicted in Milky Way globular cluster M22 (Strader et al., 2012). This supports the possibility of such a situation in nearby galaxies also.

Since the ULXs are not part of any of the correlations, our result supports the argument that the X-ray production mechanism in ULXs is different from that of the other bright X-ray sources in the galaxy emitting at lower Eddington rates. As many such sources are observed to contain spectra similar to Galactic black hole X-ray binaries, there is a probability of these sources to be black hole X-ray binaries (Angelini et al., 2001). Massive black holes emitting close to the Eddington limit can produce the observed X-ray luminosities. However, this case is statistically significant for sources with X-ray luminosities in the range 1-2 $\times$ 10^{39} erg/s (Irwin et al., 2003). The sources with luminosities higher than this limit is consistent with

the observed spatial distribution and expected numbers of back ground AGN (Ptak & Colbert, 2004). Hence, we cannot neglect AGN contamination in the study of ULXs. As ULXs are not following this relation, it is possible that their nature is completely different from the other sources of the sample. As to what could be the number and nature of X-ray emitting objects in ULXs, further studies involving more number of such objects need to be carried out. Our sample is not sufficient to draw conclusions in this regard. However, further attempts in this direction may be aided by such an observation.

SI	RA	DEC	log L_X	m_{F475W}	m_{F606W}	m_{F814W}	m_{F850LP}	Δ_g
No.	J2000	J2000	erg/s	mag	mag	mag	mag	pixels
1	3 38 38.62	-35 27 27.58	$38.53^{+0.78}_{-0.19}$	21.34 ± 0.09	–	20.15 ± 0.05	20.01 ± 0.08	2.06
2	3 38 36.83	-35 27 46.75	$38.73^{+0.31}_{-0.05}$	23.24 ± 0.21	–	22.41 ± 0.15	22.03 ± 0.21	7.87
3	3 38 36.34	-35 27 8.40	$38.43^{+0.32}_{-0.06}$	22.68 ± 0.16	–	21.39 ± 0.01	21.22 ± 0.14	7.00
4	3 38 36.30	-35 28 9.19	$38.72^{+0.12}_{-0.07}$	23.48 ± 0.24	22.66 ± 0.13	21.50 ± 0.10	21.40 ± 0.16	1.48
5	3 38 36.17	-35 26 25.11	$38.30^{+0.95}_{-0.19}$	22.43 ± 0.14	–	21.84 ± 0.12	21.39 ± 0.16	1.32
6	3 38 33.82	-35 25 56.43	$38.55^{+0.65}_{-0.12}$	20.87 ± 0.07	–	19.78 ± 0.05	19.68 ± 0.07	1.14
7	3 38 33.80	-35 26 57.96	$38.54^{+0.61}_{-0.20}$	22.82 ± 0.17	22.15 ± 0.10	21.48 ± 0.10	21.29 ± 0.15	2.95
8	3 38 33.18	-35 25 53.26	$38.44^{+0.26}_{-0.17}$	23.58 ± 0.25	–	22.18 ± 0.14	21.95 ± 0.20	2.33

Table - continued.

RA	DEC	log L_X	m_{F475W}	m_{F606W}	m_{F814W}	m_{F850LP}	Δ_g	
J2000	J2000	erg/s	mag	mag	mag	mag	pixels	
9	3 38 33.12	-35 27 31.29	$38.91^{+0.06}_{-0.04}$	21.70 ± 0.10	21.51 ± 0.08	21.07 ± 0.08	21.02 ± 0.13	1.58
10	3 38 32.80	-35 26 58.29	$38.84^{+0.17}_{-0.12}$	23.07 ± 0.20	22.62 ± 0.13	22.08 ± 0.13	21.98 ± 0.20	0.62
11	3 38 32.60	-35 27 5.12	$39.55^{+0.04}_{-0.03}$	22.16 ± 0.13	21.46 ± 0.08	20.78 ± 0.07	20.56 ± 0.11	3.93
12	3 38 32.35	-35 27 1.75	$38.91^{+0.24}_{-0.16}$	24.45 ± 0.37	23.97 ± 0.24	23.63 ± 0.27	23.58 ± 0.43	2.49
13	3 38 32.34	-35 27 10.34	$38.80^{+0.56}_{-0.14}$	23.06 ± 0.19	22.43 ± 0.12	21.74 ± 0.11	21.47 ± 0.16	3.37
14	3 38 31.90	-35 26 49.04	$38.64^{+0.13}_{-0.11}$	21.87 ± 0.11	21.83 ± 0.09	21.46 ± 0.10	21.47 ± 0.16	4.90
15	3 38 31.82	-35 26 3.760	$39.35^{+0.15}_{-0.07}$	22.80 ± 0.17	21.85 ± 0.09	21.54 ± 0.10	21.41 ± 0.16	1.93
16	3 38 29.84	-35 27 48.02	$38.54^{+0.11}_{-0.10}$	22.79 ± 0.17	22.07 ± 0.10	21.36 ± 0.09	21.15 ± 0.14	4.61

Table - continued.

RA	DEC	log L_X	m_{F475W}	m_{F606W}	m_{F814W}	m_{F850LP}	Δ_g	
J2000	J2000	erg/s	mag	mag	mag	mag	pixels	
17	3 38 27.76	-35 27 50.20	$38.94^{+0.22}_{-0.19}$	24.04 ± 0.31	24.02 ± 0.25	23.39 ± 0.24	23.32 ± 0.38	3.58
18	3 38 27.17	-35 26 0.91	$38.64^{+0.54}_{-0.15}$	22.22 ± 0.13	–	20.84 ± 0.07	20.65 ± 0.11	1.56
19	3 38 25.28	-35 27 52.97	$38.57^{+0.15}_{-0.14}$	22.26 ± 0.13	21.61 ± 0.08	20.94 ± 0.08	20.78 ± 0.12	2.53
20	3 38 31.68	-35 26 0.220	$38.52^{+0.27}_{-0.13}$	22.68 ± 0.16	–	21.23 ± 0.09	20.98 ± 0.13	3.16
21	3 38 28.96	-35 26 2.000	$38.65^{+0.10}_{-0.09}$	24.71 ± 0.42	–	23.84 ± 0.30	23.53 ± 0.42	3.18
22	3 38 25.62	-35 25 55.34	$38.71^{+0.66}_{-0.21}$	24.08 ± 0.31	–	22.81 ± 0.18	22.78 ± 0.29	2.73

Table 2.2: The table lists the properties of X-ray point sources with optical counterparts in NGC 1399. Right ascension (column 1), Declination (2) X-ray luminosity (3) apparent magnitude in *F475W* filter (4), apparent magnitude in *F555W* (5),apparent magnitude in *F606W(6)*, apparent magnitude in *F814W* (7) apparent magnitude in *F850LP*(8), and offset of X-ray source positions and their optical counterparts as observed in g band in pixels (8)

SI No.	RA	DEC	log L_X	m_{F475W} (g)	m_{F850LP} (z)	Δ_g
	J2000	J2000	erg/s	mag	mag	pixels
1	12 35 39.82	+12 33 23.0	338.5	14.841	16.572	4.23
2	12 35 39.92	+12 33 18.0	36.2	19.144	20.588	2.28
3	12 35 39.69	+12 33 18.1	28.0	18.8	20.196	2.56
4	12 35 40.30	+12 33 10.7	27.4	20.771	22.181	1.45
5	12 35 40.53	+12 33 33.3	21.9	21.761	23.058	2.43
6	12 35 40.62	+12 33 12.2	56.6	22.57	23.577	1.49
7	12 35 40.90	+12 33 17.1	34.5	22.465	-	2.96
8	12 35 39.37	+12 33 41.9	58.7	20.782	22.192	3.49
9	12 35 38.32	+12 33 18.1	14.4	21.478	22.785	1.79
10	12 35 39.69	+12 33 00.4	61.6	21.312	22.805	1.86
11	12 35 39.93	+12 33 48.1	8.3	20.023	21.491	2.23
12	12 35 38.07	+12 33 28.3	117.7	22.118	23.78	1.43
13	12 35 38.00	+12 33 37.4	15.0	22.995	-	1.22
14	12 35 38.24	+12 33 02.8	26.4	19.854	21.239	3.21

Table - continued.

SI No.	RA	DEC	log L_X	m_{F475W} (g)	m_{F850LP} (z)	Δ_g
	J2000	J2000	erg/s	mag	mag	pixels
15	12 35 40.50	+12 32 50.5	31.3	21.956	23.533	1.56
16	12 35 40.16	+12 33 58.1	34.9	21.398	22.931	2.53
17	12 35 40.99	+12 32 48.4	10.3	19.195	20.695	2.43
18	12 35 41.37	+12 32 51.1	73.2	22.505	23.908	4.33
19	12 35 42.17	+12 33 00.5	10.8	21.676	23.113	0.58
20	12 35 41.30	+12 33 59.6	29.4	20.924	22.065	1.44
21	12 35 42.39	+12 32 54.1	25.5	24.074	-	2.65
22	12 35 36.03	+12 33 33.7	37.4	20.654	21.858	1.67
23	12 35 35.25	+12 33 07.4	13.3	21.468	23.079	1.43
24	12 35 39.69	+12 34 33.1	11.3	20.485	21.949	4.07
25	12 35 44.83	+12 33 41.0	71.9	21.348	22.375	2.92
26	12 35 38.18	+12 32 03.3	15.1	21.581	23.105	2.24
27	12 35 33.69	+12 33 37.5	10.5	21.464	22.954	3.74
28	12 35 41.23	+12 34 51.7	154.0	19.275	20.51	0.55
29	12 35 41.53	+12 31 39.6	63.7	22.007	22.766	2.63

Table 2.3: The table lists the properties of X-ray point sources with optical counterparts in NGC 4552. Serial number (column 1), Right ascension (2) Declination (3) X-ray luminosity (4) apparent magnitude in *F475W* filter (5) apparent magnitude in *F850LP*(6), and offset of X-ray source positions and their optical counterparts as observed in g band in pixels (7)

SI No.	RA	DEC	log L_X	m_{F475W} (g)	$m_{F850LP}(z)$	Δ_g
	J2000	J2000	erg/s	mag	mag	pixels
1	12 43 33.34	11 32 40.00	21.97	20.70	38.86	4.23
2	12 43 41.78	11 34 33.91	23.11	22.04	38.98	2.64
3	12 43 34.83	11 32 27.72	24.65	23.25	38.75	3.77
4	12 43 35.52	11 34 27.19	22.90	21.55	38.76	2.66
5	12 43 33.96	11 34 1.15	23.09	21.58	38.73	2.35
6	12 43 31.38	11 33 2.86	22.22	21.02	38.6	1.53
7	12 43 43.61	11 33 2.97	20.06	19.74	38.52	4.12
8	12 43 38.67	11 33 4.62	21.51	20.40	38.68	3.53
9	12 43 38.92	11 32 41.25	22.16	20.84	38.65	3.21
10	12 43 39.66	11 32 48.32	24.19	23.05	38.74	3.58

Table - continued.

SI No.	RA	DEC	log L_X	m_{F475W} (g)	m_{F850LP} (z)	$g-i$	Δ_g
	J2000	J2000	erg/s	mag	mag	mag	pixels
11	12 43 41.68	11 33 51.61	22.48	20.97	38.55	2.63	
12	12 43 42.68	11 34 41.06	23.83	22.21	38.67	1.27	
13	12 43 34.71	11 32 36.99	21.44	20.03	38.4	1.77	
14	12 43 33.62	11 34 13.73	22.37	20.90	38.63	0.77	
15	12 43 41.72	11 32 18.77	22.77	21.22	38.33	1.12	
16	12 43 37.45	11 33 9.12	21.63	20.24	38.52	1.74	
17	12 43 35.86	11 34 29.70	22.33	21.29	38.54	2.13	
18	12 43 42.99	11 33 55.79	22.39	20.86	38.39	3.89	
19	12 43 33.31	11 32 29.49	23.61	22.12	38.47	2.34	

Table 2.4: The table lists the properties of X-ray point sources with optical counterparts in NGC 4649. Serial number (column 1), Right ascension (2) Declination (3) apparent magnitude in *F475W* filter (4), apparent magnitude in *F850LP* (5), X-ray luminosity (6), and offset of X-ray source positions and their optical counterparts as observed in g band in pixels (7)

Chapter 3

Study of central light concentration in nearby galaxies

3.1 Introduction

Super massive black holes (SMBHs) residing at the cores of nearby massive spheroids have been occupying the central stage in galaxy evolution studies over the past few decades. The masses of these intriguing objects scale with many of the structural and dynamical properties of their host spheroids implying the possibility of a galaxy-SMBH co-evolution.

The first among the host galaxy parameters to have shown a significant association with the SMBH masses ($M_{\rm smbh}$) was the bulge's luminosity (Kormendy & Richstone, 1995; Marconi & Hunt, 2003; Läsker et al., 2014). It was also reported that all early-type galaxies (ETGs) with $M_B \leq$ -18 host a central SMBH whose mass scales linearly with the spheroid stellar mass (Kormendy & Richstone, 1995; Ho, 1999; Hu, 2008; Sani et al., 2011). Among the series of scaling relations reported, the most influential was the discovery of the strong correlation between the black hole mass and the stellar velocity dispersion (σ) of the bulge component of the host galaxy (Ferrarese & Merritt, 2000; Gebhardt et al., 2000; Tremaine et al., 2002; Gültekin et al., 2009). Correlations of SMBH masses with the total galaxy luminosity, the concentration index of the bulge and total number of globular clusters were also noticed (Graham et al., 2001a; Graham & Driver, 2007; Burkert &

Tremaine, 2010; Beifiori et al., 2012; Savorgnan et al., 2013).

The correlations involving $M_{\rm smbh}$ and host galaxy properties seem to depend on the nature of host galaxies. Kormendy & Kennicutt (2004) suggested the existence of classical and pseudo bulges in disc galaxies and this argument was supported by various studies over the years (Kormendy et al., 2006). Classical bulges are similar in nature to elliptical galaxies and share the same fundamental plane correlation with ellipticals. They are believed to be formed in major galaxy mergers in the same way as elliptical galaxies. Pseudo bulges are more disc-like compared to classical bulges and they might have originated from secular evolution (Kormendy & Kennicutt, 2004). This distinction between the formation scenarios of the two types of bulges is supposed to be reflected in their scaling relations with $M_{\rm smbh}$. Classical bulges are correlated with $M_{\rm smbh}$ whereas pseudo bulges deviate from the correlation (Hu, 2008).

The observed correlations of SMBH masses and host galaxy properties with their negligible intrinsic scatter paved the way for an onset of theoretical studies trying to explain them. Some of them explored the possibility of an active galactic nuclei (AGN) feedback hinting at a galaxy-SMBH co-evolution (Silk & Rees, 1998; King, 2003; Fabian, 2012). Others proposed co-habitation instead of co-evolution where the correlations are governed by the merging sequence (Peng, 2007; Jahnke & Macciò, 2011).

The scaling relations are being modified over the past few years owing to the rapidly advancing techniques employed in obtaining black hole demographics. In addition to the modelling of stellar kinematics, adaptive optics and integral-field spectroscopy are also being used in the estimation of SMBH masses (Minezaki & Matsushita, 2015; Gao et al., 2017). In this light, making use of the updated SMBH masses, we attempt a photometric characterisation of the nature of SMBH hosting galaxies in the nearby Universe by studying the central three arcsec region. The photometric studies have always been limited by the effects of point spread function (PSF), and contamination by the surrounding light in the galaxy (along the line of sight). The method devised in this study is based on the concentration of optical light at the centre of the galaxy image reducing the influence of limiting factors to a minimum.

This chapter is organised as follows. Section 3.2 describes the properties of the

sample galaxies and the data reduction techniques devised in this study. Section 3.3 deals with various correlations followed by discussion and conclusion in Section 3.4.

3.2 The data

We constructed a sample of 91 galaxies from Pellegrini (2010), Kormendy & Ho (2013) and Savorgnan & Graham (2016a) subjected to the availability of the archival images by Hubble Space Telescope (HST) using Wide Field Planetary Camera 2 (WFPC2) in the *F814W* filter and SMBH mass measurements (preferably using dynamical methods) from the literature. However, we have excluded those galaxies with defects or bad pixels in the central region, or images which did not include the complete three arcsec aperture around the galaxy centre. This reduced the sample size to 49 galaxies comprising of 30 elliptical, 13 lenticular and 6 spiral galaxies. The properties of the sample galaxies are summarised in Tables 3.1 and 3.2. Spheroid masses have been adopted from Kormendy & Ho (2013). Stellar ages, total dynamical masses and half-light radii have been taken from Dabringhausen & Fellhauer (2016). The nuclear radio luminosity used in the analysis comes from Nyland et al. (2016).

3.2.1 Data Reduction

We have carried out aperture photometry (MAG_APER) using source extractor (SExtractor, Bertin & Arnouts 1996) for two circular apertures centred at the optical centre of the galaxy image. We have selected radii of 1.5 (R_1) and three (R_2) arcsecs for the inner and outer apertures respectively.

The magnitudes in the two apertures are used to calculate the intensity ratio at the centre of the galaxy image. The central intensity ratio (CIR) is defined as

$$CIR = \frac{I_1}{I_2 - I_1} = \frac{10^{0.4(m_2 - m_1)}}{1 - 10^{0.4(m_2 - m_1)}}. \tag{3.1}$$

where I_1 and I_2 are the intensities and m_1 and m_2 are the magnitudes of the light within the inner and outer apertures, respectively.

Galaxy	Dist. (Mpc)	CIR	Δ_{CIR}	$M_{\rm smbh}$ $[10^8 M_\odot]$	Ref [a]	σ (km s^{-1})
IC 1459*	28.92	0.92	0.03	24	SG16	294
IC 1481	89.90	1.11	0.08	0.149	KH13	-
IC 2560	40.7	1.44	0.09	0.044	KH13	-
IC 4296	40.7	0.78	0.02	11	SG16	327
M 31	0.774	1.27	0.03	1.4	SG16	157
M 87*	15.6	0.53	0.02	58	SG16	323
NGC 524	23.3	0.82	0.03	8.3	SG16	237
NGC 821	23.4	1.23	0.06	0.39	SG16	198
NGC 1332	22.3	0.88	0.02	14	SG16	312
NGC 1399*	19.4	0.58	0.01	4.7	SG16	334
NGC 2748	23.4	0.67	0.05	0.444	KH13	96
NGC 2778	22.3	1.53	0.12	0.15	SG16	154
NGC 2787	7.3	0.85	0.03	0.40	SG16	194

Table - continued.

Galaxy	Dist. (Mpc)	CIR	Δ_{CIR}	$M_{\rm smbh}$ [$10^8 M_\odot$]	Ref [a]	σ (km s^{-1})
NGC 2974	20.9	1.20	0.04	1.7	SG16	233
NGC 3079	20.7	0.35	0.02	0.024	SG16	175
NGC 3368	10.62	0.85	0.02	0.077	KH13	120
NGC 3377	10.9	1.41	0.04	0.77	SG16	137
NGC 3384	11.3	0.87	0.02	0.17	SG16	146
NGC 3489	11.7	1.34	0.03	0.058	SG16	105
NGC 3607*	22.2	0.67	0.02	1.3	SG16	224
NGC 3608*	22.3	1.21	0.06	2.0	SG16	193
NGC 3842*	98.4	0.91	0.05	97	SG16	309
NGC 3945	19.9	0.86	0.02	0.088	KH13	182
NGC 4026	13.2	1.21	0.05	1.8	SG16	173
NGC 4261*	30.8	0.69	0.02	5	SG16	296

Table - continued.

Galaxy	Dist. (Mpc)	CIR	Δ_{CIR}	$M_{\rm smbh}$ [$10^8 M_\odot$]	Ref [a]	σ (km s^{-1})
NGC 4278	16.1	0.89	0.03	3.39	P10	234
NGC 4291*	25.5	1.21	0.06	3.3	SG16	290
NGC 4342	23	1.80	0.07	4.5	SG16	242
NGC 4374*	18.51	0.60	0.01	9.25	KH13	275
NGC 4382*	17.88	0.92	0.02	0.130	KH13	175
NGC 4458	17.2	1.63	0.10	0.120	P10	97
NGC 4459	15.7	1.26	0.04	0.68	SG10	172
NGC 4486B	16.26	1.72	0.09	6	KH13	166
NGC 4494	17.1	1.14	0.03	0.550	P10	149
NGC 4526	16.44	0.98	0.03	4.51	KH13	224
NGC 4552	15.4	0.91	0.02	4.267	P10	250
NGC 4589	22.0	1.04	0.05	2.691	P10	219
NGC 4649*	16.46	0.50	0.01	47.2	SG16	329

Table - continued.

Galaxy	Dist. (Mpc)	CIR	Δ_{CIR}	$M_{\rm smbh}$ $[10^8 M_\odot]$	Ref [a]	σ (km s^{-1})
NGC 4889*	103.2	0.65	0.03	210	SG16	393
NGC 5018	39.4	1.16	0.03	2.09	P10	207
NGC 5516*	55.3	1.00	0.01	36.9	KH13	309
NGC 5576	24.8	1.13	0.05	1.6	SG16	182
NGC 5845	25.2	1.37	0.06	2.6	SG16	230
NGC 5846*	24.2	0.66	0.02	11	SG16	237
NGC 6251*	104.6	1.02	0.05	5	SG16	311
NGC 7052*	66.4	0.81	0.04	3.7	SG16	278
NGC 7457	12.53	1.20	0.07	0.09	KH13	68
NGC 7619*	51.5	1.02	0.04	25	SG16	316
NGC 7768*	112.8	0.66	0.04	13	SG16	288

Table 3.1: The table lists the properties of sample galaxies. Name of the galaxy (column 1), ellipticals with cores are marked with a star while the others are not, as per the classification given by Kormendy & Ho (2013), Distance (2), the CIR computed in F814W band (3), uncertainty in the estimation of the CIR (4), mass of the SMBH (5) and references for distance and mass of the SMBH (6) and stellar velocity dispersions adopted from Hyperleda (7).
References. *a*: KH13- Kormendy & Ho (2013), SG16- Savorgnan & Graham (2016b), P10- Pellegrini (2010).

Galaxy	R_e (pc)	log M_g ($M_\odot$)	log M_b ($M_\odot$)	SSP age (Gyr)	Mor. code [b]
IC 1459*	5097.3	11.67	11.6	-	1
IC 1481	-	-	-	-	6
IC 2560	9143.5	11.58	10.12	-	5
IC 4296	14189.6	11.9	-	-	1
M 31	-	-	10.35	-	4
M 87*	6414.1	11.43	11.7	17.7	1
NGC 524	4880.3	11.1	11.26	12.3	2
NGC 821	4039.6	10.79	10.98	11	2
NGC 1332	-	-	11.27	-	1
NGC 1399*	718.4	-	11.5	-	1
NGC 2748	-	-	9.41	-	5
NGC 2778	2802.2	10.2	10.26	13.4	1
NGC 2787	-	-	9.78	-	5

Table - continued.

Galaxy	R_e (pc)	log M_g ($M_\odot$)	log M_b ($M_\odot$)	SSP age (Gyr)	Mor. code [b]
NGC 2974	3309.8	10.83	-	9.3	1
NGC 3079	-	-	-	-	5[c]
NGC 3368	-	-	10.26	-	5
NGC 3377	2066.5	10.17	10.5	7	1
NGC 3384	2051.4	10.26	10.34	7.7	3
NGC 3489	1046.5	9.89	10.11	2.5	5
NGC 3607*	4713.2	11.04	11.26	10.3	6[d]
NGC 3608*	3488.5	10.65	11.01	9.9	1
NGC 3842*	12262.5	11.88	11.77	-	1
NGC 3945	3136	10.72	10.5	10.1	3
NGC 4026	1437.8	10.28	10.33	9.9	2
NGC 4261*	6892.7	11.42	11.65	16.2	1

Table - continued.

Galaxy	R_e (pc)	log M_g ($M_\odot$)	log M_b ($M_\odot$)	SSP age (Gyr)	Mor. code [b]
NGC 4278	2511.3	10.78	-	11.8	1
NGC 4291*	2400.3	11.35	10.85	-	1
NGC 4342	465.5	10.22	10.31	17.7	2
NGC 4374*	5057	11.28	11.62	14.9	1
NGC 4382*	6846.2	11.15	11.51	6.7	6
NGC 4458	1835.3	9.73	-	12	1
NGC 4459	3520.6	10.62	10.88	7	1
NGC 4486B	195.5	10.16	9.64	11.2	1
NGC 4494	3162.9	10.69	-	8	1
NGC 4526	3022	10.94	11.02	11	2
NGC 4552	3116.9	10.9	-	12.6	1
NGC 4589	6151.5	11.4	-	-	1
NGC 4649*	6173.7	11.42	11.64	17.7	1

Table - continued.

Galaxy	R_e (pc)	log M_g ($M_\odot$)	log M_b ($M_\odot$)	SSP age (Gyr)	Mor. code [b]
NGC 4889*	15005.3	12.05	12.09	2.8	1
NGC 5018	-	-	-	-	1
NGC 5516*	-	-	11.6	-	1
NGC 5576	3254.7	10.58	11	9.1	1
NGC 5845	644.7	10.19	10.57	11.5	1
NGC 5846*	7801	11.27	-	17.7	1
NGC 6251*	-	-	11.88	-	1
NGC 7052*	-	-	11.61	-	1
NGC 7457	2342	9.92	9.56	3.8	2
NGC 7619*	8375.7	11.84	11.65	15.4	1
NGC 7768*	-	-	11.75	-	1

Table 3.2: The table lists the properties of sample galaxies. Name of the galaxy (column 1), half-light radii (2) and dynamical masses of the galaxies (3) adopted from Dabringhausen & Fellhauer (2016), dynamical masses of the spheroid components of galaxies (4) adopted from Kormendy & Ho (2013), stellar age computed from population synthesis models (5) adopted from Dabringhausen & Fellhauer (2016) and morphological code (6) based on the classification by Kormendy & Ho (2013) and NED.
References. *b*: 1-ellipticals, 2-S0s with classical bulges, 3-S0s with pseudo bulges, 4-spirals with classical bulges, 5-spirals with pseudo bulges and 6-ongoing mergers; *c*: classification is given by Davis et al. (2017); *d*: classification is from Afanasiev & Silchenko (2007).

x	α	β	r	p	N
log $M_{\rm smbh}$	-1.88 ± 0.17	4.36 ± 0.17	-0.80	$>$ 99.99	33
σ	-0.38 ± 0.05	2.74 ± 0.05	-0.80	$>$ 99.99	33
$M_{\rm bulge}$	-1.41 ± 0.23	12.60 ± 0.23	-0.85	$>$ 99.99	26
$M_{\rm gal}$	-1.49 ± 0.26	12.48 ± 0.27	-0.78	$>$ 99.99	26
SSP age	-10.8 ± 1.48	22.77 ± 1.52	-0.88	$>$ 99.99	18
log $R_{\rm e}$	-0.77 ± 0.17	4.36 ± 0.17	-0.79	¿ 99.99	28
$L_{\rm radio}$	-4.01 ± 0.95	24.26 ± 0.95	-0.79	99.86	13

Table 3.3: The table lists the best-fitting parameters for the relation x = α CIR + β and correlation coefficients for various relations. N denotes the number of galaxies.

3.3 Results

The CIR is computed for the sample galaxies in F814W filter and the values are tabulated in Table 3.1. We find that the CIR is related to the properties of central SMBH and the host galaxies. We have computed linear correlation coefficients for each of the correlations listed below and these are tabulated in Table 3.3 along with the parameters used for linear fit.

3.3.1 Correlation between the CIR and $M_{\rm smbh}$

We find that the CIR of all ellipticals and classical bulges in the sample is strongly correlated with $M_{\rm smbh}$, the linear correlation coefficient, r being -0.80 with significance, p greater than 99.99 percent (Press et al., 1992). The observed anti-correlation between the CIR and $M_{\rm smbh}$ is presented in Figure 3.1(a) along with the uncertainties involved in their respective estimations. In order to explore the effect of distance on the estimation of the CIR, we tried to calculate the CIR for a range of R_1 and found it to be varying not only with the choice of R_1, but also with the

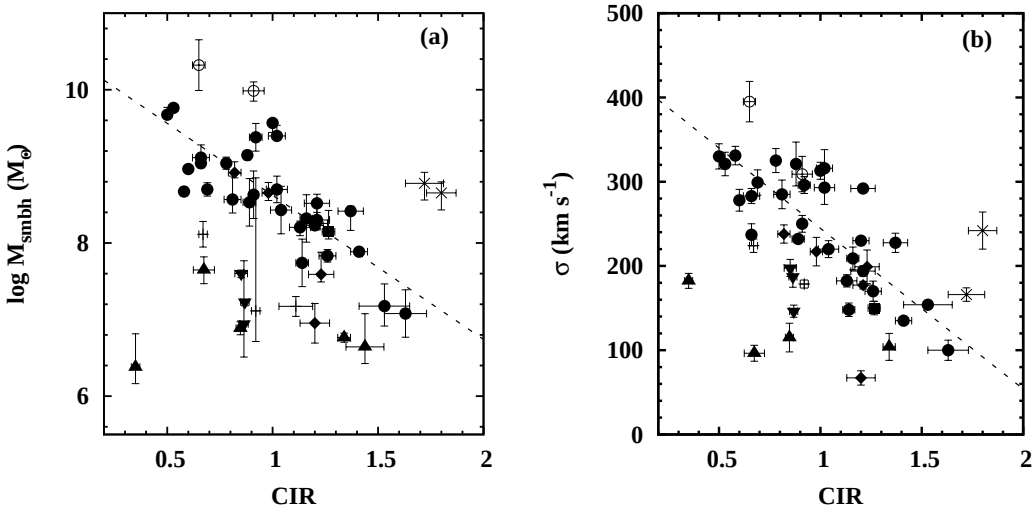

Figure 3.1: Correlation between the central intensity ratio and (a) mass of the SMBH adopted from Pellegrini (2010), Kormendy & Ho (2013) and Savorgnan & Graham (2016b) (b) stellar velocity dispersion adopted from HyperLEDA database. The best-fitting line is drawn for the sub-sample consisting of ellipticals and classical bulges. Filled circles denote elliptical galaxies, filled diamonds denote classical bulges, the square is a spiral galaxy with classical bulge, inverted triangles denote lenticular pseudo bulges, upward-pointing triangles are spiral pseudo bulges, plus marked points are galaxies with ongoing mergers, empty circles denote black hole monsters (reportedly over massive black holes residing in relatively small bulges) and cross marked points are tidally disrupted galaxies.

chosen Sérsic index, n. However, the variation is very minimum when $R_1 << R_e$ (for e.g., a variation of 0.02 when n = 3). In our sample, the R_1/R_e for the nearest and farthest galaxy is 0.008 and 0.03, respectively. Secondly, we modified R_1 (and R_2) to correspond to 1.5 (and 3) arcsecs at a distance of 16.5 Mpc (the average distance to the Virgo galaxy cluster) and redetermined the CIR. We found that the correlation coefficient did not change significantly (r = -0.79, p > 99.99 percent) even though a minor systematic offset in the CIR was observed with distance. We further confirmed that the inclusion of the five farthest galaxies (at distances > 80 Mpc) did not affect any of the correlations significantly. Hence, we have included all galaxies in our further analysis.

It can be seen that all pseudo bulges and mergers in progress deviate from the CIR-$M_{\rm smbh}$ correlation. The only galaxy with a classical bulge which does not obey the correlation is NGC 7457. Though Kormendy & Ho (2013) placed this galaxy

among classical bulges, they have not ruled out the possibility of it hosting a pseudo bulge (see section 3.4 also). Hence, the significant deviation exhibited by this galaxy might also be indicative of it hosting a dominant pseudo bulge. All other classical bulges are following the correlation between the CIR and $M_{\rm smbh}$ including the spiral galaxy M31.

In some of the SMBH-host galaxy correlations reported in the literature, it has been shown that pseudo bulges do not correlate with the mass of the black hole residing at the centre in the same way as classical bulges and ellipticals (Hu, 2008). Our result also supports this argument. In unison with pseudo bulges, mergers in progress also are found to be outliers in Figure 3.1(a). Mergers in progress are reported to be hosting black holes with underestimated masses (Kormendy & Ho, 2013). It is also possible that the deviation is indicating a different formation mechanism or a different method of accretion by the central black hole.

It might seem that the pseudo bulges and mergers in progress (denoted by triangles and plus marked points in Figure 3.1(a), respectively) excluding the edge-on spiral galaxy NGC 3379, are part of another correlation parallel to the one exhibited by ellipticals and classical bulges. This has been suggested in cases of some of the SMBH-host galaxy scaling relations (Kormendy & Ho, 2013) but our sample size of pseudo bulges is not sufficiently large to validate it. Most of the pseudo bulges which are found to deviate significantly are barred galaxies and none of the classical bulges which obey the correlation possess bars. This might be due to the secular evolution of the barred galaxies as reported by Savorgnan & Graham (2016b).

Two galaxies in our sample (NGC 4486B and NGC 4342) which are known to be tidally disrupted (Blom et al., 2014) exhibit large offsets with respect to the CIR-$M_{\rm smbh}$ relation. Also, we have not included two black hole monsters with reportedly over-massive and possibly unreliable mass estimates as suggested by Kormendy & Ho (2013) in our correlation analysis.

3.3.2 Correlations between the CIR and host galaxy properties

The CIR shows an anti-correlation (r = -0.80 with $p > 99.99$ percent) with the stellar velocity dispersion adopted from HyperLeda database as shown in Figure 3.1(b) . In this case also, the pseudo bulges are behaving differently. The two merger galaxies in our sample with the stellar velocity measurement available also deviate from the relation. The $M_{\rm smbh}$-σ correlation reported simultaneously by Ferrarese & Merritt (2000) and Gebhardt et al. (2000) is well known among the SMBH- host galaxy scaling relations. As the CIR is found to be strongly correlated with $M_{\rm smbh}$, it is not surprising to find that the former is correlated to stellar velocity dispersion as well.

We find that the CIR of ellipticals and classical bulges in the sample also shows an anti-correlation (r = -0.79, $p > 99.99$ percent) with the half-light radii of the galaxies adopted from the catalogue of ETGs compiled by Dabringhausen & Fellhauer (2016) and is shown in Figure 3.2(a). This catalogue contains $R_{\rm e}$ values estimated for different filters ranging from optical to near IR. Though this might seem to be a source of inhomogeneity, a drastic difference between $R_{\rm e}$ values estimated in g and z bands is not expected (Dabringhausen & Fellhauer, 2016) and we use it for statistical purpose alone, putting the observed scatter as an upper limit. Here also, the pseudo bulges show more scatter compared to ellipticals and classical bulges but the merger galaxies seem to be following the correlation.

It is seen that the CIR shows anti-correlation with the dynamical parameters of the galaxies such as the bulge mass ($M_{\rm bulge}$) and total dynamical mass ($M_{\rm gal}$) of the galaxy as shown in Figure 3.2(b) & 3.3(a), respectively. The bulge masses have been adopted from Kormendy & Ho (2013) while the galaxy masses are taken from Dabringhausen & Fellhauer (2016) which are estimated dynamically using $M/L_{\rm K}$ and $M/L_{\rm V}$ values, respectively. From Table 3.3, we find that $M_{\rm bulge}$ is correlated better than $M_{\rm gal}$ (r = -0.85 over 0.78) with the CIR. In the case of correlation of the CIR with $M_{\rm bulge}$, we can also find that pseudo bulges and classical bulges are clearly separated. This might be indicating an underlying connection between $M_{\rm bulge}$ and the CIR during the process of galaxy evolution. The merger galaxies in our sample obey both the correlations. We also notice that the CIR is correlated with bulge luminosities in B and V bands available from the literature but the distinction

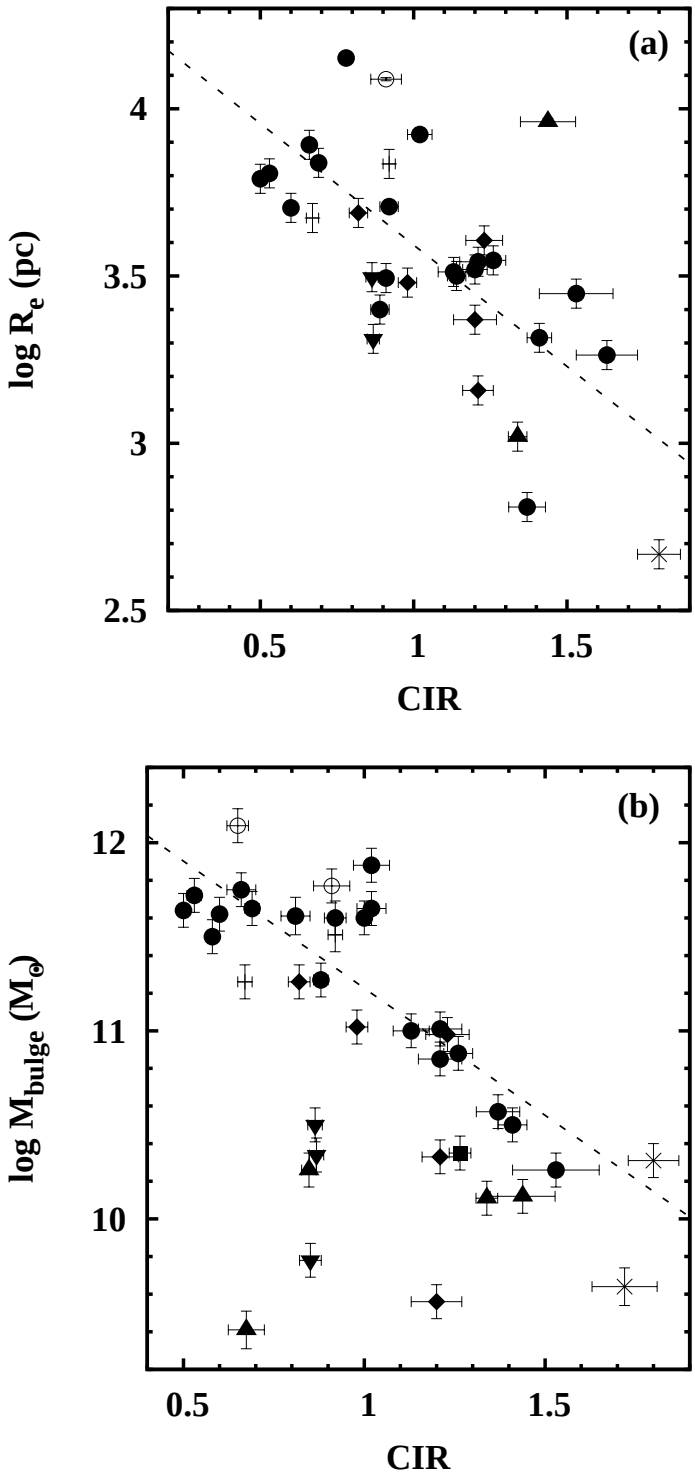

Figure 3.2: Correlations between the central intensity ratio and (a) half-light radii (R_e) adopted from Dabringhausen & Fellhauer (2016) and (b) mass of the bulge component (M_{bulge}) adopted from Kormendy & Ho (2013). The symbols denote the same objects as given in Figure 3.1

.

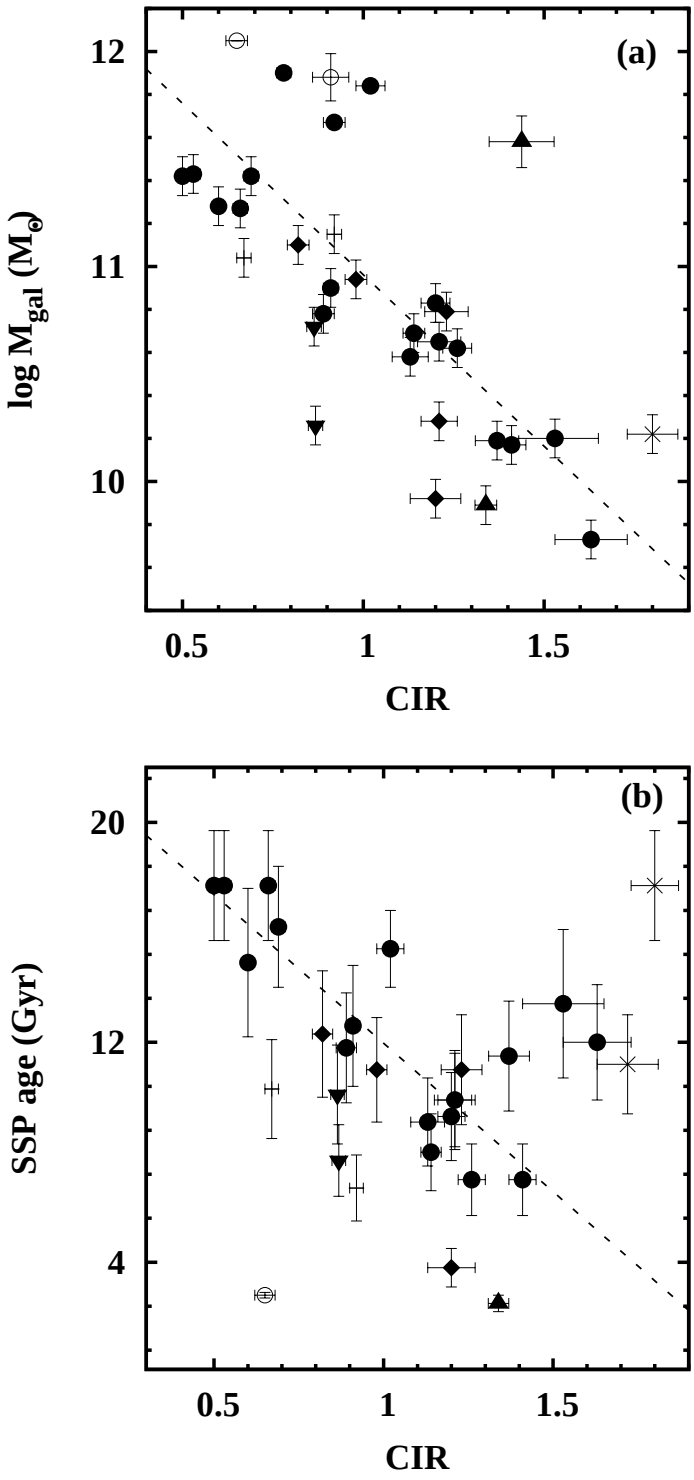

Figure 3.3: Correlations between the central intensity ratio and (a) dynamical mass of the galaxy (M_{gal}) and (d) age of the single stellar population adopted from Dabringhausen & Fellhauer (2016). The symbols denote the same objects as given in Figure 3.1

.

between classical bulges and pseudo-bulges is not evident in this case.

The stellar ages estimated using population models assuming Single Stellar Population (SSP) reported by Dabringhausen & Fellhauer (2016) are also correlated well with the CIR (r = -0.88, $p >$ 99.99 percent). Older systems are found to be possessing smaller values of the CIR as seen in Figure 3.3(b). Here also, classical bulges and pseudo bulges are clearly distinguished. The only outlier worthy of investigation is the galaxy (NGC 4889) with the highest black hole mass in the sample. Coccato et al. (2010) reported that this galaxy is found to exhibit bimodal distribution of SSP ages. According to this study, the halo of this galaxy is uniformly old with ages between 10 and 13 Gyr whereas the inner region of this galaxy is found to contain younger population. The large offset exhibited by this galaxy with respect to the relation between the CIR and SSP age might be attributed to its bimodal stellar population.

The merger galaxies NGC 4382 and NGC 3607 show notable offsets from the fitted relation between the CIR and stellar age unlike in the cases of $R_{\rm e}$, $M_{\rm bulge}$ and $M_{\rm gal}$. Here also, we find that the pseudo bulges and mergers form a parallel relation distinct from ellipticals and classical bulges. Tidally disrupted galaxies in our sample are also not following the correlation.

3.3.3 Correlation between the CIR and central radio luminosity

Nyland et al. (2016) carried out the study of nuclear radio emission in a sub-sample of ATLAS$^{\rm 3D}$ survey of ETGs using 5 GHz, Karl G. Jansky Very Large Array. They found that more than 50 percent of their sample galaxies are low luminosity AGNs (LLAGNs). We find that 16 of our galaxies are included in this study and the luminosity of their central 5 GHz radio emission is measured. Figure 3.4 shows that the CIR is strongly correlated with the central nuclear emission of these galaxies.We find that the correlation is fairly strong (r = -0.79, p = 99.86 percent) for our sample excluding the radio luminosities with only upper limits. When these points are also included, the correlation co-efficient improves to -0.84 at a significance of 99.98 percent.

The relation between SMBH masses and nuclear radio emission of ETGs is not

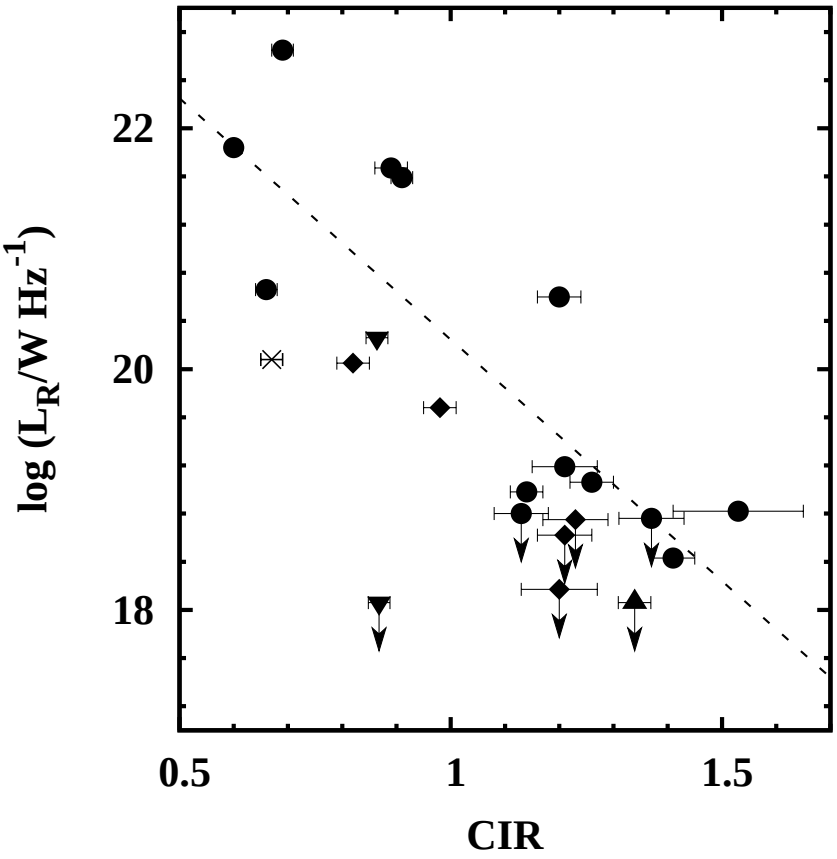

Figure 3.4: Correlation between the CIR and the central radio luminosity in 5 GHz band adopted from Nyland et al. (2016). The symbols are similar to the ones used in Figure 3.1. Downward-pointing arrows represent radio luminosity upper limits.

yet understood clearly. Some authors report that the two parameters are correlated (Nagar et al., 2005) whereas others dispute the correlation (Park et al., 2013). The current relation between optical concentration and the central radio luminosity might be indicating a co-evolution of ETGs and LLAGNs.

3.4 Discussion and conclusion

We have performed photometric studies of the centres of SMBH hosting galaxies in the nearby Universe. This study finds that the central intensity ratio (which is a newly introduced measure of the concentration of light at the very centre of the galaxy image) of ellipticals and classical bulges correlates well with the mass of the central SMBH while spirals and lenticulars with pseudo bulges deviate from the correlation. This ratio also shows significant correlations with various parameters of the SMBH hosting galaxies such as ages and masses of the stellar population. The central intensity ratio also correlates with the central radio emission from the LLAGNs reinstating its importance in studies of galaxy evolution.

The concept of optical concentration at the centre of the galaxies correlating with the mass of the SMBH is not new. Photometric parameters such as luminosity of the spheroid and stellar concentration index (Kormendy & Richstone, 1995; Graham et al., 2001a) were found to be correlated with the central SMBH masses. A series of papers were published based on the idea of concentration index which was first presented by Trujillo et al. (2001). Concentration index is defined as the ratio of flux inside some fraction α of half-light radius to the total flux within the half-light radius. This index was used by Graham et al. (2001a) to obtain a correlation between galaxy light concentration and super massive black hole mass. Graham et al. (2003) reported a strong correlation between the shape of a bulge's light profile and the mass of its central SMBH. Such studies, however, require detailed modelling of various components of the galaxies to extract their structural and photometric properties. This might require more detailed bulge-disc decomposition algorithms, which could raise the associated uncertainty levels owing to the complexity of the method. Further, the simple method used in the present study also shows similar strengths in correlations.

Graham et al. (2001b) while investigating the stability of stellar concentration

index devised in their study, speculated that the mass of the central black hole might be regulated by the way mass is distributed in a galaxy. The radii which are used in estimating the central intensity ratio in our study might not have a physical motivation. Yet, this concept seems to be significant as it appears to quantify the distribution of matter in the central region which is closely correlated with the $M_{\rm smbh}$ validating the hypothesis of Graham et al. (2001b).

Some of the galaxies in which the disc component remains embedded in the spheroid component and does not dominate the galaxy light were found to be showing large scatter in $M_{\rm smbh}$-$M_{\rm bulge}$ correlations. Recently Savorgnan & Graham (2016a) showed that some of these galaxies with intermediate-scale discs (as they are intermediate between disc-less ellipticals and disc-dominated lenticulars) have been subjected to incorrect decomposition methods. These galaxies when correctly modelled followed the correlation. The present study includes two such galaxies (NGC 1332 and NGC 4291) and these galaxies follow the observed correlation between the CIR and SMBH mass, establishing further the usefulness and significance of determination of the CIR.

We find that while ellipticals and classical bulges follow the correlation between the CIR and $M_{\rm smbh}$, pseudo bulges seem to be deviating from the correlation. The only spiral in the sample hosting a classical bulge shows the correlation whereas all other spirals hosting pseudo bulges are showing significant deviation from the observed correlation. The galaxies with ongoing mergers (NGC 3607, NGC 4382 and IC 1481) also show significant deviation.

In the case of lenticular galaxies also all classical bulges are forming an integral part of the correlation except the galaxy NGC 7457. Even though the galaxy NGC 7457 was classified to be hosting a classical bulge by Kormendy & Ho (2013), they have also discussed the possibility of it being a pseudo bulge dominant galaxy. NGC 7457 is an outlier in the correlation between the mass of the SMBH and number of globular cluster systems present in the galaxy ($M_{\rm smbh}$- $N_{\rm GC}$) reported by Harris & Harris (2011). This galaxy hosts a comparatively smaller black hole and it also has a remarkably low stellar velocity dispersion. The deviation of this particular galaxy from the observed correlation might be attributed to these reasons. Our result supports the argument that NGC 7457 might be a pseudo bulge dominant galaxy. Also, this indicates that the CIR can serve as a simple and powerful tool to

distinguish between classical bulges and pseudo bulges using photometry alone.

The fact that classical and pseudo bulges do not correlate in the same way with the mass of the super massive black hole is already established (Hu, 2008, 2009). The two types of bulges seem to follow different processes of evolution which make them differ in their scaling relations. Classical bulges are believed to be formed after major mergers. Pseudo bulges are formed secularly out of their discs (Kormendy & Kennicutt, 2004). The pseudo bulges in our sample show significant offsets from all fitted relations and our result validates this theory.

The elliptical galaxies are classified further based on their physical properties and evolution mechanisms as core-ellipticals and core-less ellipticals (Kormendy et al., 2009). Core ellipticals are believed to be formed as a result of dry mergers and these possess cuspy profiles near their centres. Core-less ellipticals are known to be formed through mergers involving star bursts at the centre thereby hosting young stellar population compared to core-galaxies (Mihos & Hernquist, 1994). Classical bulges are similar to core-less galaxies and these are generally observed to be radio-quiet (Kormendy & Ho, 2013). Our sample includes core ellipticals, core-less ellipticals and classical bulges. The CIR shows anti-correlation with the mass of the galaxy and it decreases with increasing age of the stellar population (see Figure 3.3(b)). The CIR is also anti-correlated to half light radii. We observe that all core-ellipticals in our sample with stellar ages above 14 Gyrs (except the tidally disrupted galaxy NGC 4342) have lower central intensity ratios compared to core-less galaxies such as NGC 3377 and NGC 4459. These galaxies are also radio-loud. The decrease in the central intensity ratio of these galaxies might be attributed to the dry mergers happened in the past. On the other hand, most of the classical bulges and core-less galaxies show central intensity ratios close to or more than unity. This might be due to the extra light at the centre resulting from star-bursts or wet mergers. These galaxies also contain young stellar population compared to core galaxies and many of these systems have only an upper limit to radio luminosities as seen in Figure 3.4. Hence, the CIR might also be an indicator of the evolutionary path of the galaxies.

Since the CIR-stellar age correlation is very strong and similar in nature to the CIR-$M_{\rm smbh}$ relation, the role of stellar age in establishing the CIR-$M_{\rm smbh}$ correlation needs to be explored further. However, the large uncertainties present in the data coupled with a small sample size hampers our efforts to find a plane relation between

the CIR, $M_{\rm smbh}$ and stellar age. It is also possible that the ageing population alone cannot produce the observed correlation between the CIR and SMBH masses as other factors like accretion processes by the central black hole might be contributing towards it.

We find that the central 5 GHz radio emission of LLAGNs in our sample given by Nyland et al. (2016) correlates with the central intensity ratio. The origin of this nuclear radio emission is not well understood though its origin may be linked to the synchrotron emission from the central SMBH. Another possibility proposed is the low-level circum-nuclear star formation triggers the synchrotron emission (Condon, 1992). Nyland et al. (2016) also reported a correlation between the central radio emission and SMBH mass. According to their study, the most powerful radio sources reside in ETGS with the most massive black holes. They have also discussed the possibility of the LLAGNs possessing radiatively inefficient accretion mechanisms. Since in most of the correlations listed in Section 3.3, the CIR is acting as a proxy to the black hole mass, the central radio emission might also be originating from the SMBH. Since we find that the central intensity decreases with increasing mass of the galaxy, it is quite unlikely that recent star formation occurs at the centre (Martin-Navarro et al., 2018). Many of these systems contain old stellar population which again does not support this theory. Further, more massive galaxies, in general, have large half light radii causing their centres to be less dense as seen in Misgeld & Hilker (2011). This can also result in a decrease in the central intensity ratio.

In the case of radiatively inefficient accretion as seen in ETGs, the observed scaling relations may be attributed to feedback mechanisms related to radio outflows (Heckman & Best, 2014). AGN feedback might be carried out in the form of radiative winds from energetic quasars and radio jets in LLAGNs (Ciotti et al., 2010). This feedback is capable of expelling gas from the host galaxy thereby suppressing future star formation (Morganti et al., 2013). The turbulent energy thrown out into the ambient inter stellar medium (ISM) in the form of powerful radio jets can also prevent star formation (Alatalo et al., 2015). This scenario is supported by our result as we find low values of the central intensity ratio in more massive SMBHs. It could be that the feedback mechanism is active suppressing the star formation near the central region resulting in a decrease in the CIR.

In most of the correlations listed above, the CIR seems to be on equal foot-

ing with the SMBH mass and provides a robust estimation of the SMBH masses. In this light, the advantages of using the CIR to predict SMBH masses might be highlighted. The correlations obtained using the CIR are fairly independent of the distance measurements in the nearby Universe and the central intensities. Also, simple Monte-Carlo simulations suggest that the CIR is practically independent of the viewing angle and fairly stable for relatively big ellipsoidal galaxies. This method is not expensive as we rely on photometric images for its computation. Most importantly, it is extremely simple to calculate as the procedure does not require any decomposition or modelling of the galaxy profiles and hence devoid of associated uncertainties. Also, the CIR does not depend significantly upon exposure depth of the images. Since we are dealing with ratios, redshift dependent corrections are not significant, at least in the nearby Universe. Our relation may be highly significant in case of distant galaxies as the spectroscopic measurements are difficult at high redshifts.

Chapter 4

Co-evolution of nuclear rings, bars and the central intensity ratio of their host galaxies

4.1 Introduction

Nuclear ring clusters, also known as the circum-nuclear starburst rings preferentially reside in barred spirals that constitute nearly two-thirds of the normal spirals in the local Universe (Knapen et al., 1999; Laurikainen et al., 2004). These clusters with their intense star formation activities and close association with their host galaxy's structural parameters are believed to be ideal laboratories for understanding the secular evolution of their host galaxies (Martinet, 1995; Buta & Combes, 1996; Kormendy & Kennicutt, 2004; Mazzuca et al., 2008).

The origin of the nuclear ring clusters is thought to be the gravitational torque formed as a result of the non-axisymmetric perturbations emanating from the bars, spiral arms or ovals (Shlosman, 1990; Athanassoula, 1994; Combes, 2001). The molecular gas, driven by shocks, flows inwards along the dust lanes on the leading edge of the bar and loses its angular momentum thereby spiraling into the circum-nuclear region (Kormendy & Kennicutt, 2004; Knapen, 2005). This inflow of matter can cause a burst of star formation activities and the matter gets trapped by the resonances in inner stellar orbits known as Inner Lindblad Resonances (ILRs,

Athanassoula 1994; Buta & Combes 1996; Mazzuca et al. 2008). There are various other theories about the origin of the rings such as Shlosman et al. (1990) which predicts influence of axisymmetric bulge in ring formation. Yet another explanation suggests the nuclear rings as remnants of the nuclear starbursts resulting from the high surface densities of gas in the central region (Kenney et al., 1993). Many simulations have been carried out based on various theories over the years (see e.g. Combes & Gerin, 1985; Athanassoula, 1992; Piner et al., 1995).

The nuclear ring clusters are thus believed to be tracers of star formation in such galaxies. These clusters are linked with the formation of Young Massive Clusters (YMCs) at the galaxy centres (Maoz et al., 2001; de Grijs et al., 2017). These can also be used to constrain properties of their host galaxies (Weiner & Sellwood, 1999; Li et al., 2015). Recent studies indicate that stronger bars have lower star formation at their central regions (Kim et al., 2017; Ma et al., 2018). In this light, we perform an optical study at the centres of nearby early-type spirals hosting nuclear ring clusters using a sample of 14 galaxies. We use a newly introduced parameter known as the central intensity ratio (CIR, Aswathy & Ravikumar 2018) to probe the interplay between the bars and nuclear rings in the secular evolution process.

The CIR for early-type galaxies is reported to be anti-correlated with the mass of the super massive black holes (SMBH). It is closely related to various structural and dynamical properties of host galaxies. The CIR is also found to contain information about the star formation near the central region of these galaxies. Thus, the CIR can serve as an ideal tool in studying the star forming nuclear rings. Since majority of our sample galaxies are barred, we have also explored the relation between the CIR and evolution of the bars.

This chapter is organised as follows. Section 4.2 describes the properties of the sample galaxies followed by the data reduction techniques employed in this study. Section 4.3 deals with various correlations while discussion and conclusion is provided in Section 4.4.

4.2 The data and data reduction

The sample consists of 14 early-type spiral galaxies adopted from Ma et al. (2018) hosting nuclear rings as shown in Figure 4.0 . Their sample is taken from Comerón et al. (2010) based on the primary criterion that the galaxies are observed by both *HST* and *Spitzer*. These galaxies have observations in at least four *HST* bands. Also, the sample is devoid of galaxies possessing inclination $i > 70°$ and with central regions exhibiting dusty features (Ma et al., 2018). Most of the sample galaxies possess bars except NGC 7217, NGC 7742 and UGC 3789 which helped us study the properties of the bars also. Though nuclear rings are preferentially found in barred spirals, a number of strong unbarred galaxies were also reported to host nuclear ring as seen in NGC 7742 (de Zeeuw et al., 2002). We used archival *HST* images observed using $WFPC2/ACS$ instruments in $F814W$ filter for our analysis. Out of the 17 galaxies used by Ma et al. (2018), we excluded galaxies with images that contained bad pixels in their central 3 arcsec region which restricted our sample size to 14.

The CIR for the sample galaxies is determined using simple aperture photometry (MAG_APER) provided in source extractor (*SExtractor*, Bertin & Arnouts 1996). Following Aswathy & Ravikumar (2018) we selected two circular apertures of radii of 1.5 and three arcsecs for the inner and outer regions respectively to obtain the CIR using the definition,

$$CIR = \frac{I_1}{I_2 - I_1} = \frac{10^{0.4(m_2 - m_1)}}{1 - 10^{0.4(m_2 - m_1)}}. \tag{4.1}$$

where, I_1 and I_2 are the intensities and m_1 and m_2 are the magnitudes of the light enclosed by the inner and outer apertures, respectively. The properties of the sample galaxies are provided in Table 4.1. The relative sizes and lengths of the semi-major axis of nuclear rings are adopted from Comerón et al. (2010) while other parameters are taken from Ma et al. (2018). We have also listed the values of CIR along with their uncertainties in Table 4.1.

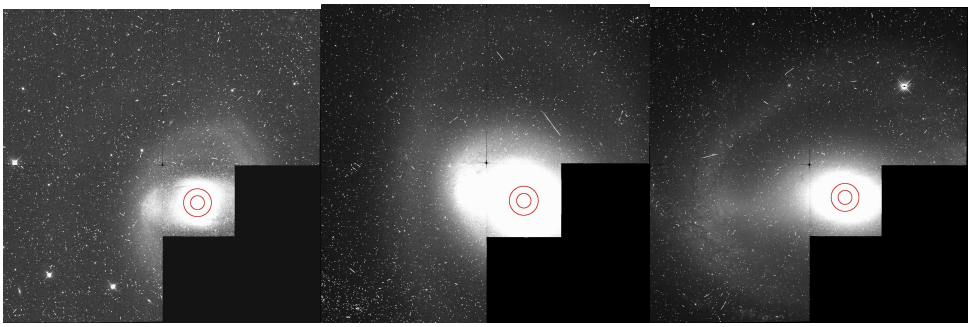

(a) ESO 565-11 (b) NGC 1326 (c) NGC 1512

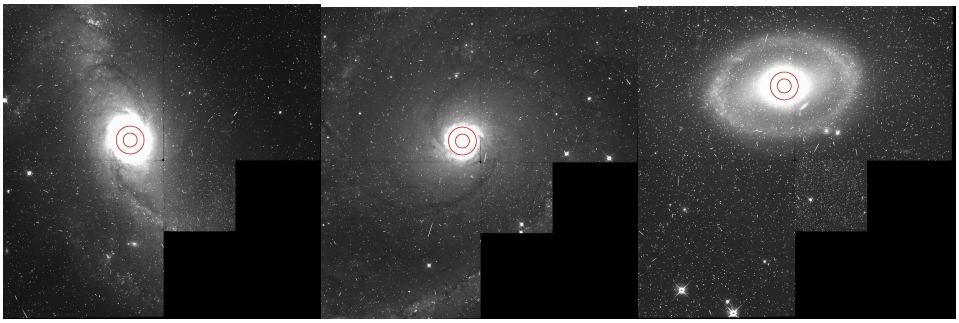

(d) NGC 1672 (e) NGC 2997 (f) NGC 3081

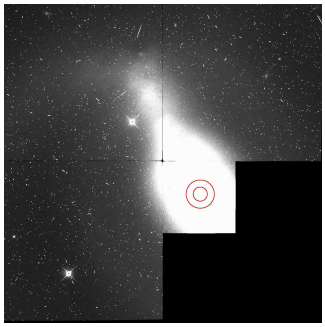

(g) NGC 4314

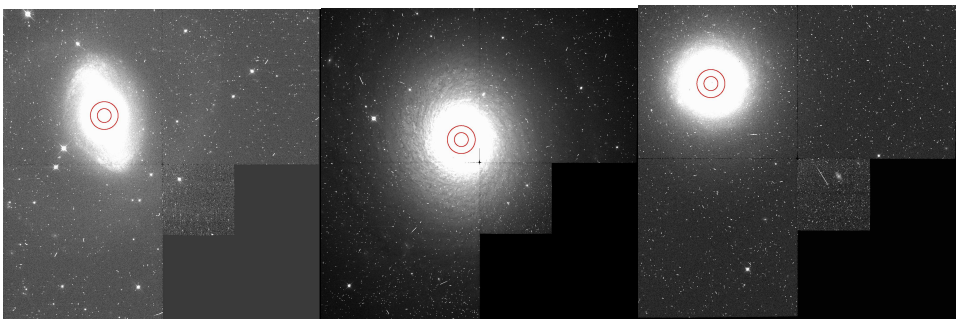

(h) NGC 6782 (i) NGC 7217 (j) NGC 7742

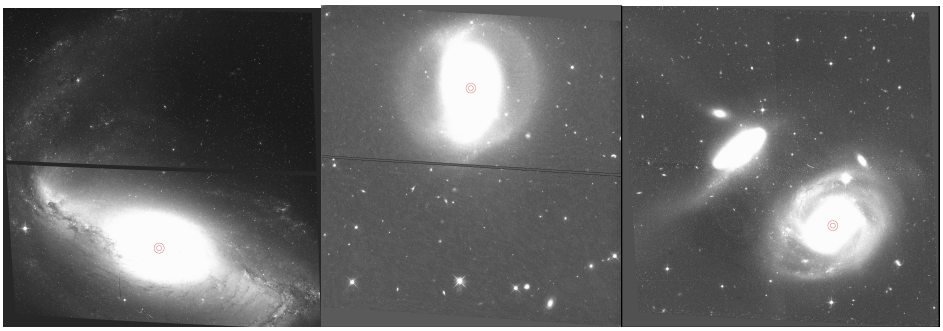

(k) NGC 1097 (l) UGC 3789 (m) NGC 7469

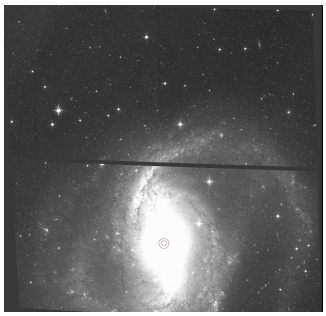

(n) NGC 6951

Figure 4.0: The *HST* images of the 14 spiral galaxies listed in Table 4.1. Overlaid are 1.5″ and 3″ circles centred on the optical centre of the galaxy image. Note that all the galaxies are face on with inclination, $i > 70°$.

Galaxy	Hubble type	M-m (mag)	Q_g	f	Σ (kpc^{-2})	D_r/D_0	a_r (pc)	CIR	Δ_{CIR}
ESO 565-11	(R)SB(r)0/a	34.23	0.316	0.77	8	0.212	3560	1.29	0.15
NGC 1097	SB(s)b	31.4	0.241	0.55	213	0.041	970	0.77	0.01
NGC 1326	(R)SB0+(r)	30.86	0.163	0.56	484	0.048	480	0.85	0.02
NGC 1512	SB(r)a	30.48	0.366	0.33	363	0.052	480	0.67	0.03
NGC 1672	SB(s)b	30.81	0.349	0.3	3020	0.031	420	0.76	0.02
NGC 2997	SAB(rs)c	30.2	0.306	0.57	179	0.016	350	0.83	0.04
NGC 3081	(R)SAB(r)0/a	32.09	0.194	0.63	18	0.094	1200	0.88	0.04
NGC 4314	SB(rs)a	29.93	0.432	0.82	565	0.061	560	0.91	0.04
NGC 6782	(R)SAB(r)a	33.61	0.205	0.92	7	0.06	1150	1.09	0.05
NGC 6951	SAB(rs)bc	31.77	0.275	0.79	108	0.034	560	0.73	0.03
NGC 7217	(R)SA(r)ab	31.41	0.026	0.64	49	0.082	840	0.97	0.03
NGC 7469	(R')SAB(rs)a	34.07	0.049	0.81	61	0.047	700	1.06	0.01
NGC 7742	SA(r)b	32.91	0.055	0.61	22	0.163	1050	1.20	0.06
UGC 3789	(R)SA(r)ab	33.49	—	0.77	39	—	—	0.97	0.02

Table 4.1: The table lists the properties of sample galaxies. Name of the galaxy (column 1), Hubble Type (2) and Distance modulus (3) non-axisymmetric torque parameter Q_g (4), ratio of the number of final ring cluster population to the initial ring cluster population (5), and surface densities of ring clusters (6) taken from Ma et al. (2018), relative size of the ring (7) and semi major axis of the ring (8) adopted from Comerón et al. (2010), the CIR computed in $F814W$ band (9), uncertainty in the estimation of the CIR (10).

x	α	β	r	p	N
Q_g	-0.51 ± 0.12	0.67 ± 0.11	-0.88	99.64	10
f	1.38 ± 0.21	-0.60 ± 0.19	-0.91	99.94	11
Σ	-3.04 ± 0.81	4.79 ± 0.77	-0.77	99.64	12
D_r/D_{25}	0.24 ± 0.05	-0.15 ± 0.04	-0.80	99.67	13
a_r	1.05 ± 0.27	1.91 ± 0.26	-0.81	99.74	13

Table 4.2: The table lists the best-fitting parameters for the relation x = α CIR + β and N denotes the number of galaxies following it. The linear correlation coefficient (r) is listed along with the significance (p).

4.3 Results

We find that the CIR is closely associated with various properties of nuclear rings. We also explore connections between the CIR and bar strengths of these galaxies. The linear correlation coefficients for all major correlations are given in Table 4.2 along with the values of the best-fitting parameters.

4.3.1 Correlations between the CIR and the properties of nuclear rings

Nuclear rings are believed to be closely associated with the activities in the central region of host galaxies and its stellar population (Sarzi et al., 2007; Mazzuca et al., 2008; Ma et al., 2018). Evolution of a ring is found to depend on the dynamics of the (associated) bar also (Buta et al., 1999; Comerón et al., 2010). Yet, the photometric studies carried out so far seldom observed a direct connection between the properties of the ring and its host galaxy. In the present study, we find a strong correlation between the CIR and the relative size of the ring (D_r/D_o), adopted from Comerón et al. (2010), as shown in Figure 4.1(a). The linear correlation coefficient, r, is -0.88 with a significance, p, of 99.64 percent (Press et al., 1992). The relative size of the

ring denotes the size of the ring normalised with the detection threshold for *HST* (2 arcsec). This parameter is reported to be connected with the non-axisymmetric perturbation strength (Comerón et al., 2010) and is further discussed in section 4.3.2 .

The semi-major axis length of the ring (a_r) also correlates well with the CIR positively, the correlation coefficient being 0.80 with a significance over 99 percent as seen in Figure 4.1(b). The uncertainties in the measurement of semi major axis length are reported to depend on the orientation parameters used for fitting ellipses to various images (such as Hα and UV). Further, this parameter is obtained assuming that the nuclear ring lie in the galactic plane of the disc, which might not be the case always (Comerón et al., 2010). The scatter in the correlation between the CIR and a_r might have originated from these elements of uncertainty.

In addition, we find that the fraction of the number of objects in the final selected ring cluster to that of the initial ring cluster obtained in Ma et al. (2018) is strongly connected with the CIR barring three outliers as shown in Figure 4.2(a). Two of the outliers in this plot are unbarred galaxies (NGC 7742 and NGC 6951) and these show different properties in most of the correlations listed in Ma et al. (2018). The third galaxy ESO 565-11 hosts a highly elliptical ring which is currently being formed (Buta et al., 1999). This galaxy is also found to be an outlier in many of the correlations exhibited by galaxies hosting nuclear rings (Comerón et al., 2010). Finally, we see that the ring cluster surface densities are anti-correlated with the values of CIR hinting of a close association of the CIR with the formation and evolution of the rings (see Figure 4.2(b)). There are two notable outliers, the first being NGC 4314, the youngest member of the sample which is reported to be behaving differently (Ma et al., 2018). The second outlier NGC 1672 is known to be heavily obscured by dust (Diaz et al., 2001) which might have contributed to the uncertainty in its ring cluster surface density estimations.

4.3.2 Correlation between the CIR and the strength of the bar

The non-axisymmetric torque parameter (Q_g) was first defined by Combes & Sanders (1981) as the ratio of the maximum tangential force to the mean radial force and

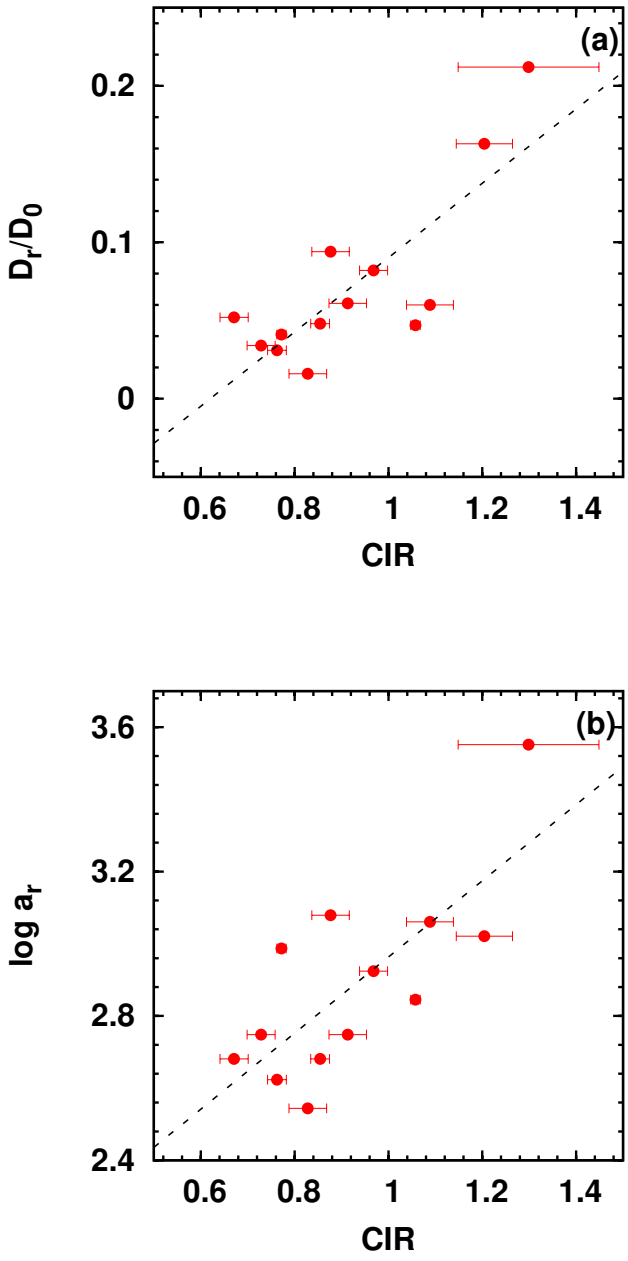

Figure 4.1: Correlations between the central intensity ratio and (a) relative size of the ring, D_r/D_o, the ratio of the diameter of the ring to the *HST* detection threshold (b) logarithm of the semi major axis of the ring measured in parsec, a_r, adopted from Comerón et al. (2010). The red coloured circles represent the galaxies following the fitted relations and outliers are denoted by blue triangles.

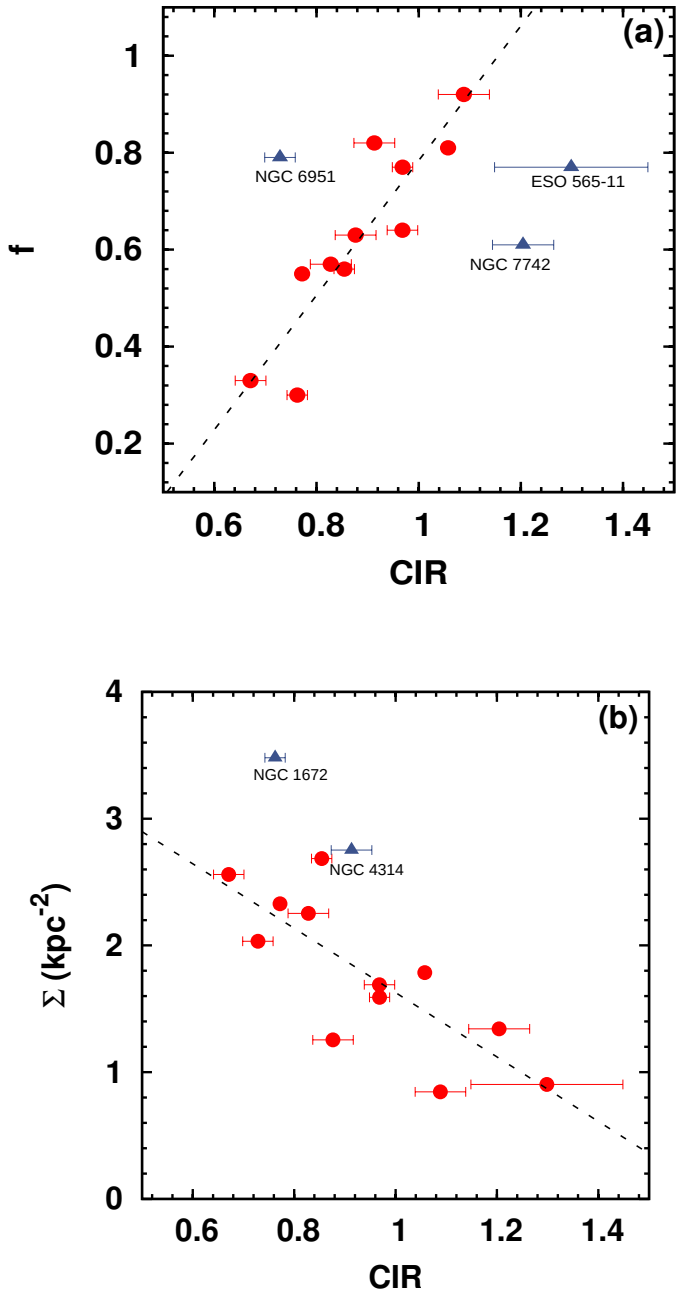

Figure 4.2: Correlations between the central intensity ratio and (a) the fraction of number of objects in the final ring cluster to the initial cluster, f and (b) ring cluster surface density, Σ, taken from Ma et al. (2018). The red coloured circles represent the galaxies following the fitted relations and outliers are denoted by blue triangles.

it quantifies the strength of the bar. Higher values of Q_g indicate stronger bars while lower values might be attributed to arm perturbations and oval distortions (Comerón et al., 2010). In the case of galaxies without bars, this parameter may statistically be related to the strength of the spiral arms (Ma et al., 2018). We find a striking anti-correlation (r= -0.88 with p= 99.64 percent) between the CIR and Q_g as shown in Figure 4.3. Three galaxies (NGC 4314, NGC 7217 and ESO 565-11) show significant offsets with respect to the fitted relation between the CIR and Q_g. The galaxy NGC 7217 is an unbarred galaxy. This galaxy is known to contain a counter rotating stellar disc unlike the other galaxies in the sample (Comerón et al., 2010). Mazzuca et al. (2008) proposed that this galaxy might have under gone a minor merger in the past with a gas-rich dwarf galaxy. The peculiarities of the other two outliers are already discussed in section 4.3.1. The strong correlation between the bar strength and the CIR probably reflects the bar-driven star formation in the sample galaxies.

4.4 Discussion and conclusion

We perform photometric studies of the centres of 14 early-type spirals (majority with bars) in the nearby Universe hosting nuclear ring clusters. We use the CIR, a recently introduced measure of the concentration of light at the very centre of the galaxy image to study the formation and evolution of the nuclear ring clusters and their host galaxies. The CIR is found to be a significant parameter in galaxy evolution studies as it is correlated with many structural and dynamical properties of early-type galaxies including the mass of the SMBH at the centre (Aswathy & Ravikumar, 2018). However, estimation of CIR is not straight forward for spiral galaxies due to orientation effects posed by the disc component. But in the present study of spiral galaxies with nuclear rings, the orientation of most of the galaxies are face-on ($i > 70°$) enabling us to neglect the orientation effects induced by dust present in disc. Also, early-type spirals are known to be less heavily obscured by dust compared to late-type spirals (Comerón et al., 2010). Further, these galaxies are situated within 80 Mpcs and hence do not require distance induced corrections in the estimation of CIR (Aswathy & Ravikumar, 2018). These features of our sample helped us unveil, for the first time, striking photometric correlations between the

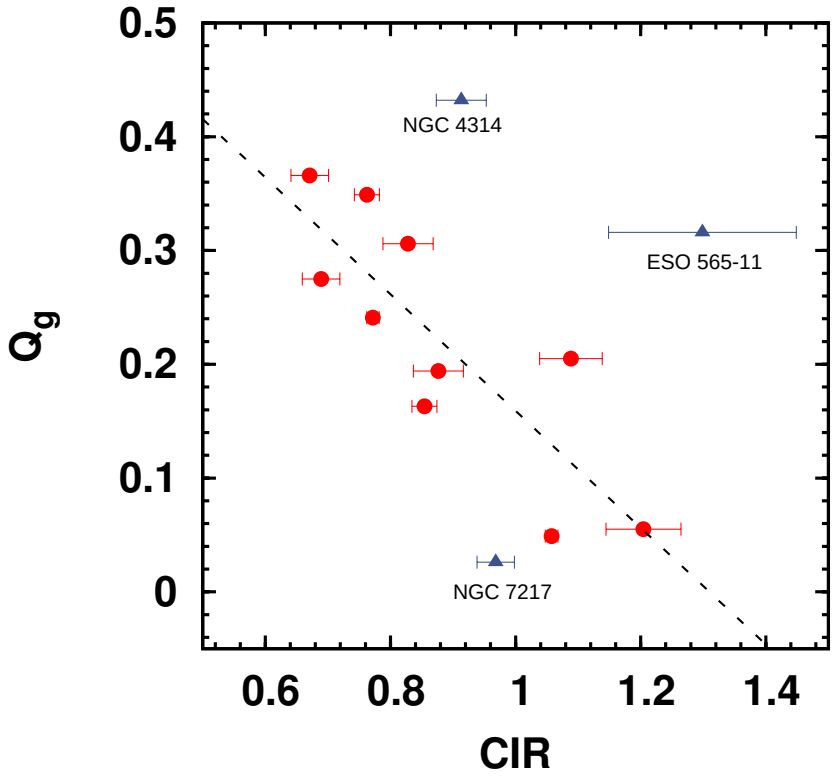

Figure 4.3: Correlation between the CIR and non-axisymmetric torque parameter (Q_g) adopted from Ma et al. (2018). The symbols are similar to those used in Figure 4.1

properties of nuclear rings and the CIR of their host galaxies. Also, we find that the bar strength of the sample galaxies is strongly correlated with the CIR reinstating the importance of the latter in galaxy evolution studies.

The present study indicates that the CIR is lower in strongly barred galaxies compared to the weak ones as quantified by the non-axisymmetric torque parameter. We know that the stellar bars in nearby spirals play a major role in the secular evolution of their host galaxies as they are capable of redistributing gaseous matter from the discs to inner regions of the galaxy (Sanders & Huntley, 1976; Athanassoula, 1992). Such an infall of materials might trigger starbursts at the galactic centres (Ho et al., 1997; Hunt & Malkan, 1999). Several observational and theoretical studies dealing with the bar-driven star formation in spirals suggest that this enhancement in star formation activity near the central region occurs at the onset of bar formation (e.g. Heckman, 1980; Ellison et al., 2011; Fanali et al., 2015; Spinoso et al., 2017). Once the bar is formed, the star formation starts declining and by the time the bar grows stronger, the star formation gets suppressed (Spinoso et al., 2017; Abdurro'uf & Akiyama, 2017).

The CIR contains information regarding the star formation activities near the central region of early-type galaxies (Aswathy & Ravikumar, 2018). As seen in Figure 4.3, the CIR decreases with the increasing strength of bars. The lower values of the CIR suggest that the star formation at the centre is minimum compared to the outer regions. This might be the result of the bar sweeping out the gaseous matter as it gets stronger and this is consistent with previous studies (James & Percival, 2018). Recently, Ma et al. (2018) investigated the star formation rates of barred spirals and arrived at the same conclusion.

Also, we find that various properties of the nuclear rings correlate with the CIR. The smaller rings are found to possess lower values of the CIR as seen in Figure 4.1(a). The semi major axis of the rings is also found to be increasing with the CIR. The ring cluster surface density is anti-correlated with the CIR, re-affirming that in the galaxies with small and dense rings, the star formation activities at the centre is reduced. This might be a consequence of bar controlled evolution of nuclear rings (see for e.g. Knapen 2005). Many simulations also suggest that smaller rings occur in strongly barred galaxies (e.g. Kim et al., 2014). Knapen (2005) propose that the nuclear rings can shrink as the bar gets stronger which seems to support our

observation.

The ratio of the number of star clusters in the final ring to that in the initial ring also seems to be increasing with the CIR. When the CIR is small, we see that more clusters are present in the central region of the galaxy which might be indicating a migration of clusters from outer to inner regions of galaxies as suggested by van de Ven & Chang (2009). According to this study, if the formed star clusters in the ring are massive and more in number, coupled with a lower mass inflow rate at the centre, the nuclear ring can migrate closer to the centres of the host galaxy. The low values of CIR suggest high cluster surface density and compact rings as seen in Figures 4.2(b) and 4.1(a) respectively. This also indicates the presence of stronger bars and thereby lesser star formation. In short, the CIR shows intimate relations with the evolution of the nuclear rings and has the prospect of being used as an effective tool in their study.

The CIR is reported to be anti-correlated with the mass of the central SMBH in early-type galaxies. So far, studies have not been successful in unveiling any direct observational correlation between the active galactic nucleus (AGN) activities and occurrence of bars or formation of nuclear rings. The absence of intense star formation in the central region and strong AGN activities may be due to the prompt removal of gas in the central region (Ho et al., 1997; Hunt & Malkan, 1999; Knapen et al., 2000; Laine et al., 2002). Recently, a numerical simulation exploring the AGN feedback and star formation history in barred spiral galaxies proposed that after the initial star burst, as a result of the inflowing gas materials towards the central AGN, the gas is gradually pushed away from the galactic centres shifting the star formation sites to larger radii (Robichaud et al., 2017). This scenario is also supported in the present study as we find low values of central intensity ratios in strong bars. In the case of early-type systems, it was observed that low values of central intensity ratio suggest massive black holes in galactic centres (Aswathy & Ravikumar, 2018). Thus, the CIR seems to possess the potential to play a crucial role in understanding the linked evolution of rings, bars and central AGNs.

Chapter 5

Summary and future plans

Studies on galaxy evolution are significant in Astronomy as these help unfold crucial information regarding the dynamical evolution of the Universe. Ever since the pioneering morphological classification of galaxies by Edwin Hubble, various studies revealed intense connections between morphology and population of galaxies. The evolution of many classes of objects such as X-ray point sources and super massive black holes was found to be depending on their host galaxy morphology. Hence, studying a group of galaxies which are morphologically similar and devising correlations between various parameters might prove fruitful in understanding their dynamical evolution. In this light, we perform studies on nearby galaxies using photometric techniques.

In Chapter 1, we give a brief introduction to the work presented in this thesis. The first part of our work deals with the study of optical counterparts of the bright X-ray sources in nearby early-type galaxies. The other two parts of the work concern with photometric studies on the central regions of galaxies. Chapter 1 includes a brief literature review so as to illustrate the significance of each of these works in the current scenario. We explain the motivation behind our work and present a brief outline of the thesis. We have also discussed about the telescopes which provided us with the images used in our study. Further, the softwares used in our analysis are also introduced.

The second chapter describes the work on the optical counterparts of bright X-ray point sources in nearby early-type galaxies. Our sample consists of bright X-ray

sources in three nearby galaxies: NGC 1399, NGC 4552 and NGC 4649. We identify the optical counterparts of these sources with the help of SExtractor and *IRAF* and perform aperture photometry of these sources in different filters. Further, we carry out the stellar population synthesis of these sources to estimate their dynamical ages and masses. The main results obtained from this work are listed below.

- The X-ray luminosities are strongly anti-correlated with $F475W - F850LP$ colours for non-Ultraluminous sources in all three galaxies of the sample.
- ULXs included in the sample clearly defy the correlation suggesting that the mechanism of X-ray production in ULXs may be different from the other bright X-ray sources.
- The masses of these sources obtained from SPS analysis are also found to be anti-correlated with the X-ray luminosities. Here also, the ULXs behave differently.
- The ages of the clusters indicate that the brighter X-ray sources are younger compared to the less brighter sources.
- As the optical counterparts are definitely multiple sources (most likely globular clusters), the strong trend exhibited by X-ray sources suggests the possibility of existence of multiple sources for the production of X-rays as well.

Chapter 3 is an account of the study on the central light concentration in nearby early-type galaxies. We devise a new tool termed as the central intensity ratio (CIR) which is found to be intimately connected with the galaxy evolution. We use a sample of 49 galaxies with known black hole masses to unveil a significant connection between the CIR and mass of the central super massive black holes. The main results of this work can be summarised as follows.

- We find that the CIR of ellipticals and classical bulges is found to be strongly correlated with SMBH masses whereas pseudobulges and ongoing mergers show significant scatter.

- The CIR of low luminosity active galactic nuclei (LLAGN) in the sample shows significant connection with the 5 GHz nuclear radio emission suggesting a stronger link between the former and the SMBH evolution in these galaxies.
- In addition, it is seen that various structural and dynamical properties of the SMBH host galaxies are correlated with the CIR making the latter an important parameter in galaxy evolution studies.
- We propose the CIR to be an efficient and simple tool not only to distinguish classical bulges from pseudo bulges but also to estimate the mass of the central SMBH.

In the last part of the work which is described in Chapter 4, we carry out a study on nuclear rings in nearby spirals using the method of CIR. The sample consists of 14 early-type spiral galaxies adopted from Ma et al. (2018) hosting nuclear rings. Nuclear rings are believed to be closely associated with the activities in the central region of host galaxies and its stellar population (Sarzi et al., 2007; Mazzuca et al., 2008; Ma et al., 2018). Evolution of a ring is found to depend on the dynamics of the (associated) bar also (Buta et al., 1999; Comerón et al., 2010). Yet, the photometric studies carried out so far seldom observed a direct connection between the properties of the ring and its host galaxy. In the present work, we find that the CIR is closely associated with various properties of nuclear rings. We also explore connections between the CIR and bar strengths of these galaxies. The results of this work are summarised below.

- We observe that the relative sizes and lengths of the semi major axis of nuclear rings strongly correlate with the CIR.
- These correlations suggest that the galaxies hosting smaller and denser nuclear rings may have little star formation near their centres as these tend to possess low values of CIR.
- This scenario appears to be a consequence of stronger bars as advocated by the significant connection observed between the CIR and bar strengths.
- The CIR can serve as a crucial parameter in unfolding the coupled evolution of bars and rings as it is intimately connected with both their properties.

5.0.1 Future scopes of the work

- Our work on the optical counterparts of X-ray point sources in nearby galaxies can be further explored with the help of spectroscopic study of individual star clusters which is currently being carried out. This will give us one more dimension to probe into the dynamics of the system.
- We also plan to extend this work to a larger sample if and when the data are available.
- The ULXs are exhibiting unique properties which demand for further exploration. We plan to carry out a study on ULXs alone and attempt to study the stellar population residing in them.
- The correlation between black hole mass and the CIR obtained in the study of central light concentration of galaxies can be revised as more and more independent black hole mass estimations become available.
- We plan to extend the study of central light concentration to a sample of AGNs. In our sample, we had observed a correlation between the CIR and central radio emission of low luminosity AGNs.
- The present work is performed in the optical region. This can be extended to IR and UV wavelengths to study how the CIR varies in different regions of electromagnetic spectrum.

Bibliography

Abdurro'uf, & Akiyama, M. 2017, MNRAS, 469, 2806

Afanasiev, V. L., & Silchenko, O. K. 2007, Astronomical and Astrophysical Transactions, 26, 311

Alatalo, K., Lacy, M., Lanz, L., et al. 2015, ApJ, 798, 31

Angelini, L., Loewenstein, M., & Mushotzky, R. F. 2001, ApJ, 557, L35

Ashman, K. M., & Zepf, S. E. 1998, Globular Cluster Systems

Aswathy, S., & Ravikumar, C. D. 2018, MNRAS, 477, 2399

Athanassoula, E. 1992, MNRAS, 259, 328

Athanassoula, E. 1994, in Mass-Transfer Induced Activity in Galaxies, ed. I. Shlosman, 143

—. 2002, Ap&SS, 281, 39

Barmby, P., McLaughlin, D. E., Harris, W. E., Harris, G. L. H., & Forbes, D. A. 2007, AJ, 133, 2764

Beifiori, A., Courteau, S., Corsini, E. M., & Zhu, Y. 2012, MNRAS, 419, 2497

Bellazzini, M., Pasquali, A., Federici, L., Ferraro, F. R., & Pecci, F. F. 1995, ApJ, 439, 687

Bertin, E., & Arnouts, S. 1996, A&AS, 117, 393

Blakeslee, J. P., Cho, H., Peng, E. W., et al. 2012, ApJ, 746, 88

Blom, C., Forbes, D. A., Foster, C., Romanowsky, A. J., & Brodie, J. P. 2014, MNRAS, 439, 2420

Brodie, J. P., & Strader, J. 2006, ARA&A, 44, 193

Bruzual, G., & Charlot, S. 2003, MNRAS, 344, 1000

Bruzual A., G., & Charlot, S. 1993, ApJ, 405, 538

Burkert, A., & Tremaine, S. 2010, ApJ, 720, 516

Buta, R., & Combes, F. 1996, Fund. Cosmic Phys., 17, 95

Buta, R., Crocker, D. A., & Byrd, G. G. 1999, AJ, 118, 2071

Cappellari, M., Renzini, A., Greggio, L., et al. 1999, ApJ, 519, 117

Chabrier, G. 2003, PASP, 115, 763

Charlot, S., Worthey, G., & Bressan, A. 1996, ApJ, 457, 625

Ciotti, L., Ostriker, J. P., & Proga, D. 2010, ApJ, 717, 708

Clark, G. W. 1975, ApJ, 199, L143

Coccato, L., Gerhard, O., & Arnaboldi, M. 2010, MNRAS, 407, L26

Colbert, E. J. M., & Mushotzky, R. F. 1999, ApJ, 519, 89

Combes, F. 2001, in Astronomical Society of the Pacific Conference Series, Vol. 230, Galaxy Disks and Disk Galaxies, ed. J. G. Funes & E. M. Corsini, 213–220

Combes, F., & Gerin, M. 1985, A&A, 150, 327

Combes, F., & Sanders, R. H. 1981, A&A, 96, 164

Comerón, S., Knapen, J. H., Beckman, J. E., et al. 2010, MNRAS, 402, 2462

Condon, J. J. 1992, ARA&A, 30, 575

Dabringhausen, J., & Fellhauer, M. 2016, MNRAS, 460, 4492

D'Abrusco, R., Fabbiano, G., Mineo, S., et al. 2014, ApJ, 783, 18

Davis, B. L., Graham, A. W., & Seigar, M. S. 2017, MNRAS, 471, 2187

de Grijs, R., Ma, C., Jia, S., Ho, L. C., & Anders, P. 2017, MNRAS, 465, 2820

de Zeeuw, P. T., Bureau, M., Emsellem, E., et al. 2002, MNRAS, 329, 513

Devi, A. S., Misra, R., Agrawal, V. K., & Singh, K. Y. 2007, ApJ, 664, 458

Diaz, R., Dottori, H., & Carranza, G. 2001, in Revista Mexicana de Astronomia y Astrofisica, vol. 27, Vol. 11, Revista Mexicana de Astronomia y Astrofisica Conference Series, 137

Dunn, L. P., & Jerjen, H. 2006, AJ, 132, 1384

Ellison, S. L., Nair, P., Patton, D. R., et al. 2011, MNRAS, 416, 2182

Fabbiano, G. 1989, ARA&A, 27, 87

—. 2006, ARA&A, 44, 323

Faber, S. M. 1972, A&A, 20, 361

Fabian, A. C. 2012, ARA&A, 50, 455

Fanali, R., Dotti, M., Fiacconi, D., & Haardt, F. 2015, MNRAS, 454, 3641

Feng, H., & Soria, R. 2011, New A Rev., 55, 166

Ferrarese, L., & Merritt, D. 2000, ApJ, 539, L9

Filho, M. E., Barthel, P. D., & Ho, L. C. 2000, ApJS, 129, 93

Forbes, D. A., Beasley, M. A., Brodie, J. P., & Kissler-Patig, M. 2001, ApJ, 563, L143

Forbes, D. A., Raul Faifer, F., Carlos Forte, J., et al. 2004, MNRAS, 355, 608

Gao, F., Braatz, J. A., Reid, M. J., et al. 2017, ApJ, 834, 52

Gebhardt, K., & Kissler-Patig, M. 1999, AJ, 118, 1526

Gebhardt, K., Bender, R., Bower, G., et al. 2000, ApJ, 539, L13

Giacconi, R., Branduardi, G., Briel, U., et al. 1979, ApJ, 230, 540

Gilfanov, M. 2004, MNRAS, 349, 146

Graham, A. W. 2008, ApJ, 680, 143

Graham, A. W., & Driver, S. P. 2007, ApJ, 655, 77

Graham, A. W., Erwin, P., Caon, N., & Trujillo, I. 2001a, ApJ, 563, L11

Graham, A. W., Erwin, P., Caon, N., & Trujillo, I. 2003, in Revista Mexicana de Astronomia y Astrofisica Conference Series, Vol. 17, Revista Mexicana de Astronomia y Astrofisica Conference Series, ed. V. Avila-Reese, C. Firmani, C. S. Frenk, & C. Allen, 196–197

Graham, A. W., Trujillo, I., & Caon, N. 2001b, AJ, 122, 1707

Grindlay, J. E., Hertz, P., Steiner, J. E., Murray, S. S., & Lightman, A. P. 1984, ApJ, 282, L13

Gültekin, K., Richstone, D. O., Gebhardt, K., et al. 2009, ApJ, 698, 198

Harris, G. L. H., & Harris, W. E. 2011, MNRAS, 410, 2347

Harris, J., Calzetti, D., Gallagher, III, J. S., Conselice, C. J., & Smith, D. A. 2001, AJ, 122, 3046

Harris, W. E., Allwright, J. W. B., Pritchet, C. J., & van den Bergh, S. 1991, ApJS, 76, 115

Heckman, T. M. 1980, A&A, 88, 365

Heckman, T. M., & Best, P. N. 2014, ARA&A, 52, 589

Ho, L. 1999, in Astrophysics and Space Science Library, Vol. 234, Observational Evidence for the Black Holes in the Universe, ed. S. K. Chakrabarti, 157

Ho, L. C., Filippenko, A. V., & Sargent, W. L. W. 1997, ApJS, 112, 315

Hu, J. 2008, MNRAS, 386, 2242

—. 2009, ArXiv e-prints

Humphrey, P. J., & Buote, D. A. 2008, ApJ, 689, 983

Hunt, L. K., & Malkan, M. A. 1999, ApJ, 516, 660

Iben, Jr., I., Tutukov, A. V., & Fedorova, A. V. 1997, ApJ, 486, 955

Irwin, J. A. 2005, ApJ, 631, 511

Irwin, J. A., Athey, A. E., & Bregman, J. N. 2003, ApJ, 587, 356

Irwin, J. A., Bregman, J. N., & Athey, A. E. 2004, ApJ, 601, L143

Ivanova, N., Rasio, F. A., Lombardi, Jr., J. C., Dooley, K. L., & Proulx, Z. F. 2005, ApJ, 621, L109

Jahnke, K., & Macciò, A. V. 2011, ApJ, 734, 92

James, P. A., & Percival, S. M. 2018, MNRAS, 474, 3101

Jithesh, V., Misra, R., Shalima, P., et al. 2014, Research in Astronomy and Astrophysics, 14, 1251

Jones, L. A., & Worthey, G. 1995, ApJ, 446, L31

Jordán, A., Côté, P., Ferrarese, L., et al. 2004, ApJ, 613, 279

Jordán, A., Sivakoff, G. R., McLaughlin, D. E., et al. 2007, ApJ, 671, L117

Juett, A. M. 2005, ApJ, 621, L25

Kaaret, P., Feng, H., & Roberts, T. P. 2017, ARA&A, 55, 303

Kenney, J. D. P., Carlstrom, J. E., & Young, J. S. 1993, ApJ, 418, 687

Kim, D.-W., & Fabbiano, G. 2010, ApJ, 721, 1523

Kim, D.-W., Fabbiano, G., Ivanova, N., et al. 2013, ApJ, 764, 98

Kim, E., Hwang, H. S., Chung, H., et al. 2017, ApJ, 845, 93

Kim, E., Kim, D.-W., Fabbiano, G., et al. 2006, ApJ, 647, 276

Kim, W.-T., Seo, W.-Y., & Kim, Y. 2014, in IAU Symposium, Vol. 303, The Galactic Center: Feeding and Feedback in a Normal Galactic Nucleus, ed. L. O. Sjouwerman, C. C. Lang, & J. Ott, 43–53

King, A. 2003, ApJ, 596, L27

King, A. R., Davies, M. B., Ward, M. J., Fabbiano, G., & Elvis, M. 2001, ApJ, 552, L109

Knapen, J. H. 2005, A&A, 429, 141

Knapen, J. H., Laine, S., & Relaño, M. 1999, Ap&SS, 269, 605

Knapen, J. H., Pérez-Ramírez, D., & Laine, S. 2002, MNRAS, 337, 808

Knapen, J. H., Shlosman, I., & Peletier, R. F. 2000, ApJ, 529, 93

Körding, E., Falcke, H., & Markoff, S. 2002, A&A, 382, L13

Kormendy, J. 1982, ApJ, 257, 75

Kormendy, J., & Bender, R. 2012, ApJS, 198, 2

Kormendy, J., Bender, R., & Cornell, M. E. 2011, Nature, 469, 374

Kormendy, J., Cornell, M. E., Block, D. L., Knapen, J. H., & Allard, E. L. 2006, ApJ, 642, 765

Kormendy, J., Fisher, D. B., Cornell, M. E., & Bender, R. 2009, ApJS, 182, 216

Kormendy, J., & Gebhardt, K. 2001, in American Institute of Physics Conference Series, Vol. 586, 20th Texas Symposium on relativistic astrophysics, ed. J. C. Wheeler & H. Martel, 363–381

Kormendy, J., & Ho, L. C. 2013, ARA&A, 51, 511

Kormendy, J., & Kennicutt, Jr., R. C. 2004, ARA&A, 42, 603

Kormendy, J., & Richstone, D. 1995, ARA&A, 33, 581

Kundu, A., Maccarone, T. J., & Zepf, S. E. 2002, ApJ, 574, L5

—. 2007, ApJ, 662, 525

Kundu, A., Maccarone, T. J., Zepf, S. E., & Puzia, T. H. 2003, ApJ, 589, L81

Kundu, A., & Whitmore, B. C. 2001, AJ, 122, 1251

Laine, S., Shlosman, I., Knapen, J. H., & Peletier, R. F. 2002, ApJ, 567, 97

Larsen, S. S., Forbes, D. A., & Brodie, J. P. 2001, MNRAS, 327, 1116

Läsker, R., Ferrarese, L., van de Ven, G., & Shankar, F. 2014, ApJ, 780, 70

Laurikainen, E., Salo, H., Buta, R., & Vasylyev, S. 2004, MNRAS, 355, 1251

Le Borgne, J.-F., Bruzual, G., Pelló, R., et al. 2003, A&A, 402, 433

Li, Z., Shen, J., & Kim, W.-T. 2015, ApJ, 806, 150

Long, K. S., Dodorico, S., Charles, P. A., & Dopita, M. A. 1981, ApJ, 246, L61

Ma, C., de Grijs, R., & Ho, L. C. 2018, ArXiv e-prints

Maccarone, T. J., Kundu, A., & Zepf, S. E. 2003, ApJ, 586, 814

—. 2004, ApJ, 606, 430

Madau, P., & Rees, M. J. 2001, ApJ, 551, L27

Maoz, D., Barth, A. J., Ho, L. C., Sternberg, A., & Filippenko, A. V. 2001, AJ, 121, 3048

Marconi, A., & Hunt, L. K. 2003, ApJ, 589, L21

Martin-Navarro, I., Brodie, J. P., Romanowsky, A. J., Ruiz-Lara, T., & van de Ven, G. 2018, Nature, 553, 307

Martinet, L. 1995, Fund. Cosmic Phys., 15, 341

Mazzuca, L. M., Knapen, J. H., Veilleux, S., & Regan, M. W. 2008, ApJS, 174, 337

Mieske, S., JordÃąn, A., CÃťtÃĺ, P., et al. 2010, ApJ, 710, 1672

Mihos, J. C., & Hernquist, L. 1994, ApJ, 437, L47

Miller, M. C., & Hamilton, D. P. 2002, ApJ, 576, 894

Mineo, S., Fabbiano, G., D'Abrusco, R., et al. 2014, ApJ, 780, 132

Minezaki, T., & Matsushita, K. 2015, ApJ, 802, 98

Minniti, D., Rejkuba, M., Funes, J. G., & Akiyama, S. 2004, ApJ, 600, 716

Misgeld, I., & Hilker, M. 2011, MNRAS, 414, 3699

Morganti, R., Fogasy, J., Paragi, Z., Oosterloo, T., & Orienti, M. 2013, Science, 341, 1082

Mukai, K., Pence, W. D., Snowden, S. L., & Kuntz, K. D. 2003, ApJ, 582, 184

Nagar, N. M., Falcke, H., & Wilson, A. S. 2005, A&A, 435, 521

Nyland, K., Young, L. M., Wrobel, J. M., et al. 2016, MNRAS, 458, 2221

Ostrov, P. G., Forte, J. C., & Geisler, D. 1998, AJ, 116, 2854

Paolillo, M., Puzia, T. H., Goudfrooij, P., et al. 2011, ApJ, 736, 90

Park, S., Sohn, B. W., & Yi, S. K. 2013, A&A, 560, A80

Peacock, M. B., Maccarone, T. J., Waters, C. Z., et al. 2009, MNRAS, 392, L55

Peacock, M. B., & Zepf, S. E. 2016, ApJ, 818, 33

Pellegrini, S. 2010, ApJ, 717, 640

Peng, C. Y. 2007, ApJ, 671, 1098

Peng, E. W., Jordán, A., Côté, P., et al. 2006, ApJ, 639, 95

Pickles, A. J. 1985, ApJ, 296, 340

Pierce, M., Bridges, T., Forbes, D. A., et al. 2006, MNRAS, 368, 325

Piner, B. G., Stone, J. M., & Teuben, P. J. 1995, ApJ, 449, 508

Press, W. H., Teukolsky, S. A., Vetterling, W. T., & Flannery, B. P. 1992, Numerical recipes in FORTRAN. The art of scientific computing

Ptak, A., & Colbert, E. 2004, ApJ, 606, 291

Randall, S. W., Sarazin, C. L., & Irwin, J. A. 2004, ApJ, 600, 729

Roberts, T. P., & Warwick, R. S. 2000, MNRAS, 315, 98

Roberts, T. P., Fabbiano, G., Luo, B., et al. 2012, ApJ, 760, 135

Robichaud, F., Williamson, D., Martel, H., Kawata, D., & Ellison, S. L. 2017, MNRAS, 469, 3722

Salpeter, E. E. 1955, ApJ, 121, 161

Sanders, R. H., & Huntley, J. M. 1976, ApJ, 209, 53

Sani, E., Marconi, A., Hunt, L. K., & Risaliti, G. 2011, MNRAS, 413, 1479

Sarazin, C. L., Irwin, J. A., & Bregman, J. N. 2000, ApJ, 544, L101

Sarzi, M., Allard, E. L., Knapen, J. H., & Mazzuca, L. M. 2007, MNRAS, 380, 949

Savorgnan, G., Graham, A. W., Marconi, A., et al. 2013, MNRAS, 434, 387

Savorgnan, G. A. D., & Graham, A. W. 2016a, MNRAS, 457, 320

—. 2016b, ApJS, 222, 10

Serra, P., & Oosterloo, T. A. 2010, MNRAS, 401, L29

Shih, I. C., Charles, P. A., & Cornelisse, R. 2011, MNRAS, 412, 120

Shlosman, I. 1990, in NASA Conference Publication, Vol. 3098, NASA Conference Publication, ed. J. W. Sulentic, W. C. Keel, & C. M. Telesco

Shlosman, I., Begelman, M. C., & Frank, J. 1990, Nature, 345, 679

Silk, J., & Rees, M. J. 1998, A&A, 331, L1

Sivakoff, G. R., Jordán, A., Sarazin, C. L., et al. 2007, ApJ, 660, 1246

Smits, M., Maccarone, T. J., Kundu, A., & Zepf, S. E. 2006, A&A, 458, 477

Spinoso, D., Bonoli, S., Dotti, M., et al. 2017, MNRAS, 465, 3729

Strader, J., Chomiuk, L., J Maccarone, T., Miller-Jones, J., & C Seth, A. 2012, 490, 71

Swartz, D. A., Ghosh, K. K., Tennant, A. F., & Wu, K. 2004, ApJS, 154, 519

Swartz, D. A., Soria, R., Tennant, A. F., & Yukita, M. 2011, ApJ, 741, 49

Tinsley, B. M. 1978, ApJ, 222, 14

Trager, S. C., Faber, S. M., Worthey, G., & González, J. J. 2000, AJ, 120, 165

Tremaine, S., Gebhardt, K., Bender, R., et al. 2002, ApJ, 574, 740

Trinchieri, G., & Fabbiano, G. 1985, ApJ, 296, 447

Trujillo, I., Graham, A. W., & Caon, N. 2001, MNRAS, 326, 869

van de Ven, G., & Chang, P. 2009, ApJ, 697, 619

Vazdekis, A. 1999, ApJ, 513, 224

Verbunt, F., & Hut, P. 1987, in IAU Symposium, Vol. 125, The Origin and Evolution of Neutron Stars, ed. D. J. Helfand & J.-H. Huang, 187

Voss, R., & Gilfanov, M. 2006, in IAU Symposium, Vol. 230, Populations of High Energy Sources in Galaxies, ed. E. J. A. Meurs & G. Fabbiano, 364–368

Weinberg, M. D. 1985, MNRAS, 213, 451

Weiner, B. J., & Sellwood, J. A. 1999, ApJ, 524, 112

Worthey, G., Faber, S. M., Gonzalez, J. J., & Burstein, D. 1994, ApJS, 94, 687

Xu, Y., Xu, H., Zhang, Z., et al. 2005, ApJ, 631, 809

Yi, S. K. 2003, ApJ, 582, 202

Young, L. M., Rosolowsky, E., van Gorkom, J. H., & Lamb, S. A. 2006, ApJ, 650, 166

Zhang, Z., Gilfanov, M., & Bogdán, Á. 2012, A&A, 546, A36